Electronic Supporting Information

Contents

1. Syntheses

1.1. Synthesis of *cyclo*-{$P_4{}^tBu_3(SiMe_3)$}

257.6 mg **1** (0.525 mmol) were suspended in 3 ml Et_2O and 0.08 ml $SiClMe_3$ (0.629 mmol, 1.20 equiv.) were added. All volatiles were removed under reduced pressure and the residue was dried *in vacuo* at 40 °C for 10 min. The residue was extracted with 10 ml *n*-hexane. Removing the solvent under reduced pressure yielded 188.3 mg (0.511 mmol, 97 % yield, spectroscopic purity 95 %). Literature reports a synthesis with 18 % yield.[1]

2. Crystallography

Compound	**1**	**3**	**4**	**5**	**6†**	**7**	**8**
Empirical formula	$C_{22}H_{51}LiN_2OP_4$	$C_{28}H_{63}P_9$	$C_{25}H_{56}P_8$	$C_{36}H_{81}BiP_{12}$	$C_{36}H_{81}P_{12}Sb$	$C_{36}H_{81}AsP_{12}$	$C_{24}H_{54}AsClP_8$
Formula weight	490.46	678.51	604.45	1094.62	1007.39	960.56	700.80
Temperature [K]	130(2)	130(2)	240(2)	130(2)	130(2)	130(2)	130(2)
Wavelength [pm]	71.073	71.073	71.073	71.073	71.073	71.073	71.073
Crystal system	Monoclinic	Triclinic	Monoclinic	Monoclinic	Monoclinic	Monoclinic	Triclinic
Space group	$P2_1$	$P\bar{1}$	$P2_1$/n	$P2_1$/c	$P2_1$/c	$P2_1$/c	$P\bar{1}$
Unit cell							
a [pm]	887.51(2)	982.83(2)	1300.38(3)	1409.55(2)	1401.71(2)	1383.40(2)	903.35(4)
b [pm]	1546.65(3)	1348.69(3)	1821.42(4)	2388.32(3)	2376.66(3)	2348.73(2)	1333.30(4)
c [pm]	1119.23(3)	1516.21(3)	1623.94(4)	1619.85(2)	1627.34(2)	1642.33(2)	1658.76(6)
α [deg]	90	84.231(2)	90	90	90	90	68.090(3)
β [deg]	105.434(3)	82.229(2)	108.890(3)	100.8960(10)	100.9570(10)	101.0980(10)	83.488(3)
γ [deg]	90	77.488(2)	90	90	90	90	81.416(3)
Volume [nm^3]	1.48093(6)	1.93876(7)	3.6392(2)	5.3548(1)	5.3225(1)	5.2365(1)	1.8292(1)
Z	2	2	4	4	4	4	2
ρ (calc) [Mg/m^3]	1.100	1.162	1.103	1.358	1.257	1.218	1.272
μ mm^{-1}	0.270	0.418	0.396	3.674	0.902	1.039	1.365
F(000)	536	732	1304	2240	2112	2040	736
Crystal size (mm^3)	0.40 x 0.25 x 0.15	0.25 x 0.20 x 0.10	0.35 x 0.30 x 0.20	0.39 x 0.08 x 0.05	0.70 x 0.11 x 0.08	0.40 x 0.30 x 0.25	0.30 x 0.20 x 0.10
Θ min / *Θ* max [deg]	1.888 / 32.561	2.368 / 34.907	1.734 / 29.213	1.705 / 30.258	1.958 / 32.303	2.293 / 32.689	2.285 / 32.508
Index ranges	$-13 \le h \le 13$ $-23 \le k \le 22$ $-16 \le l \le 16$	$-15 \le h \le 15$ $-20 \le k \le 21$ $-24 \le l \le 23$	$-16 \le h \le 17$ $-24 \le k \le 24$ $-22 \le l \le 20$	$-18 \le h \le 19$ $-31 \le k \le 32$ $-21 \le l \le 22$	$-20 \le h \le 21$ $-35 \le k \le 35$ $-24 \le l \le 23$	$-20 \le h \le 19$ $-34 \le k \le 35$ $-23 \le l \le 24$	$-13 \le h \le 13$ $-20 \le k \le 19$ $-24 \le l \le 23$
Reflections collected	19005	56622	33109	57685	40984	78078	40036
Independent reflections [R(int)]	9687 [0.0318]	15839 [0.0188]	8716 [0.0429]	14673 [0.0538]	40984 [0.0518]	17694 [0.0458]	12182 [0.0366]
Completeness [%] (*Θ*) [deg]	100.0 (30.510)	99.96 (33.070)	100.0 (26.375)	100.0 (28.285)	100.0 (30.510)	100.0 (30.510)	100.0 (30.510)
T_{Max} / T_{Min}	1.00000 / 0.78300	1.00000 / 0.96568	1.00000 / 0.68495	1.00000 / 0.69643	1.00000 / 0.92965	1.00000 / 0.98587	1.00000 / 0.95830
Restraints / parameters	1 / 284	0 / 355	0 / 316	0 / 469	0 / 470	0 / 469	0 / 344
Goodness-of-fit on F^2	1.028	1.062	1.013	1.023	0.802	1.044	1.121

R_1, wR_2 [$I > 2\sigma(I)$]	0.0384, 0.0798	0.0245, 0.0593	0.0450, 0.1033	0.0359, 0.0654	0.0363, 0.0549	0.0348, 0.0678	0.0415, 0.0741
R indices (all data)	0.0491, 0.0861	0.0316, 0.0626	0.0884, 0.1231	0.0533, 0.0710	0.0827, 0.0595	0.0577, 0.0760	0.0621, 0.0798
Absolute structure parameter	0.00(3)	–	–	–	–	–	–
Residual electron density [e·Å^{-3}]	0.229 / –0.297	0.415 / –0.229	0.364 / –0.240	1.117 / –1.001	1.053 / –1.142	0.418 / –0.412	0.353 / –0.309
CCDC number	2097486	2097387	2097487	2097488	2097489	2097490	2097491

† Two component twin. Twin law by rows –0.50 –0.50 –0.25, 1.50 –0.50 0.25, 0.00 0.00 1.00; Twin domain ratio: 0.9358(1) : 0.0642(1)

3. NMR Spectra

All spectra were recorded in C_6D_6 at 25 °C unless stated otherwise.

3.1. [Li{*cyclo*-($P_4{}^tBu_3$)}(thf)(tmeda)] (1)

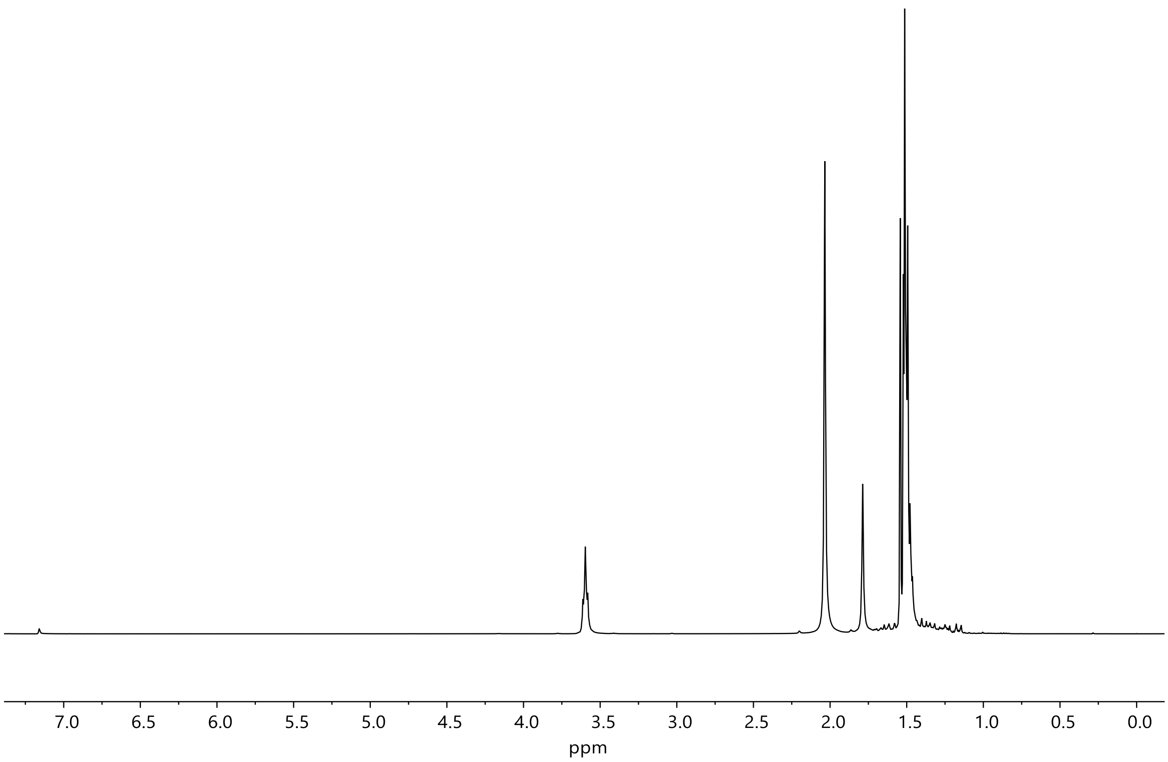

Fig. S1 ^{1}H NMR spectrum of **1** at 400 MHz.

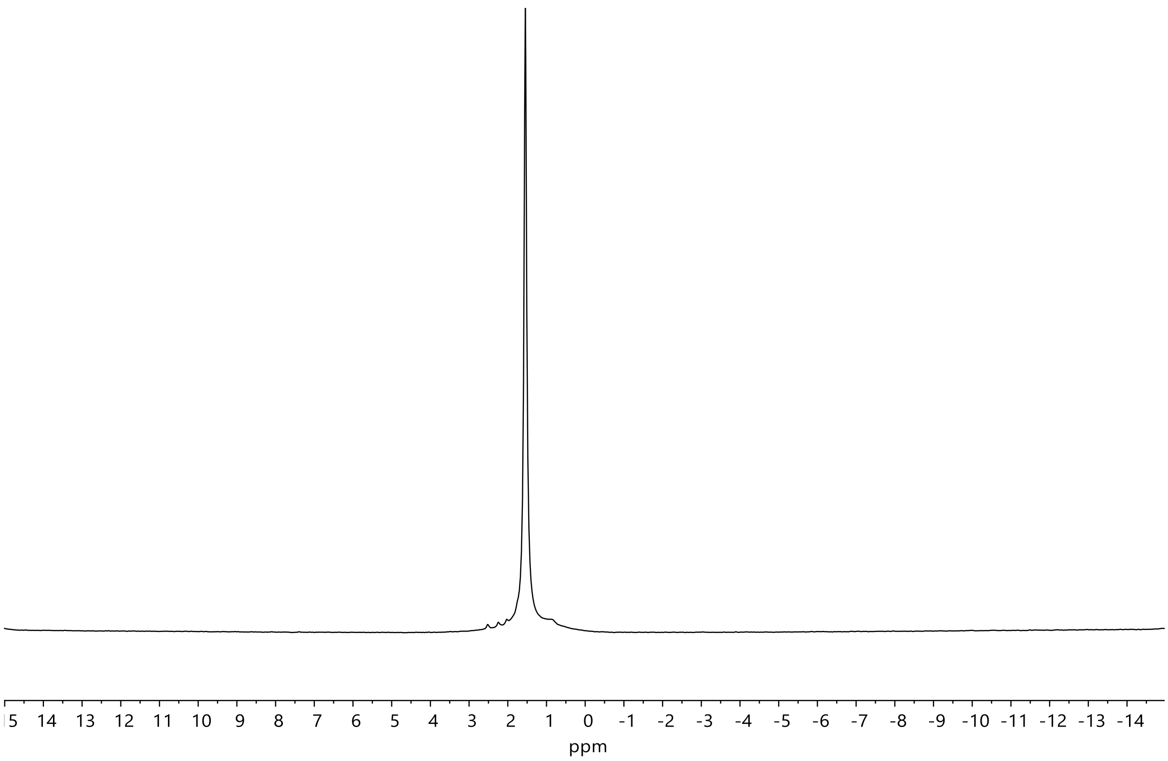

Fig. S2 $^{7}Li\{^{1}H\}$ NMR spectrum of **1** at 156 MHz.

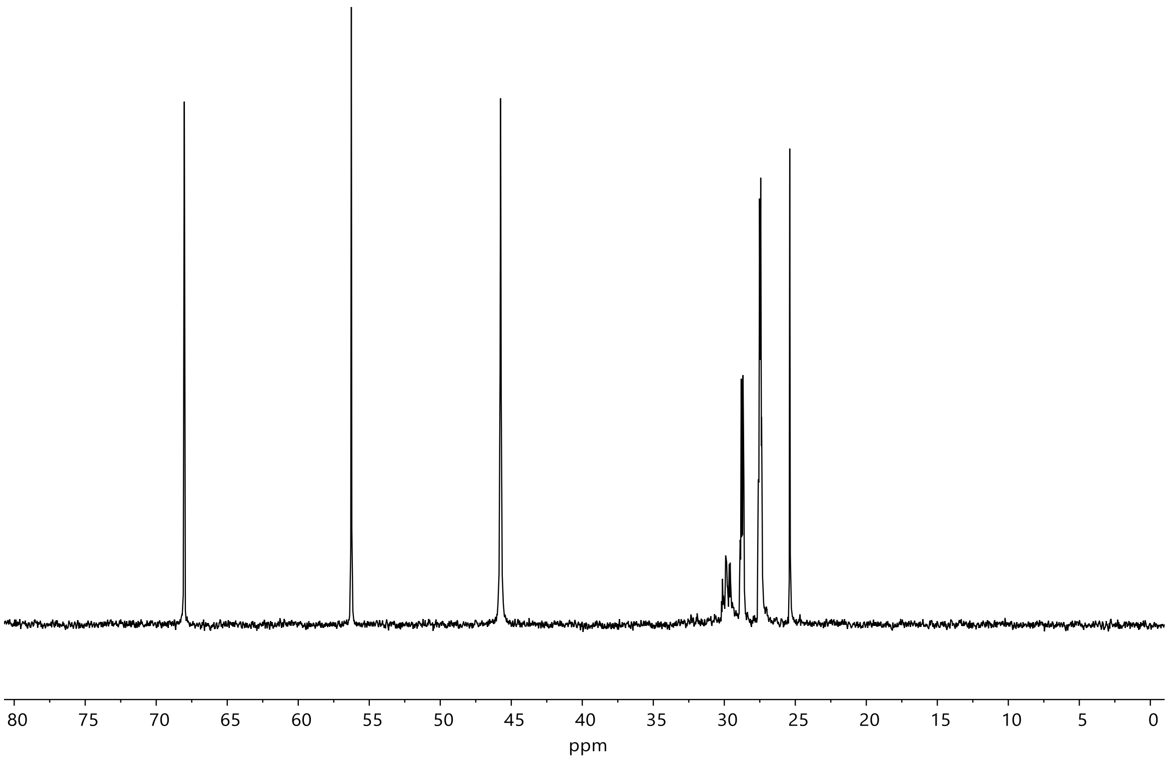

Fig. S3 $^{13}C\{^{1}H\}$ NMR spectrum of **1** at 101 MHz.

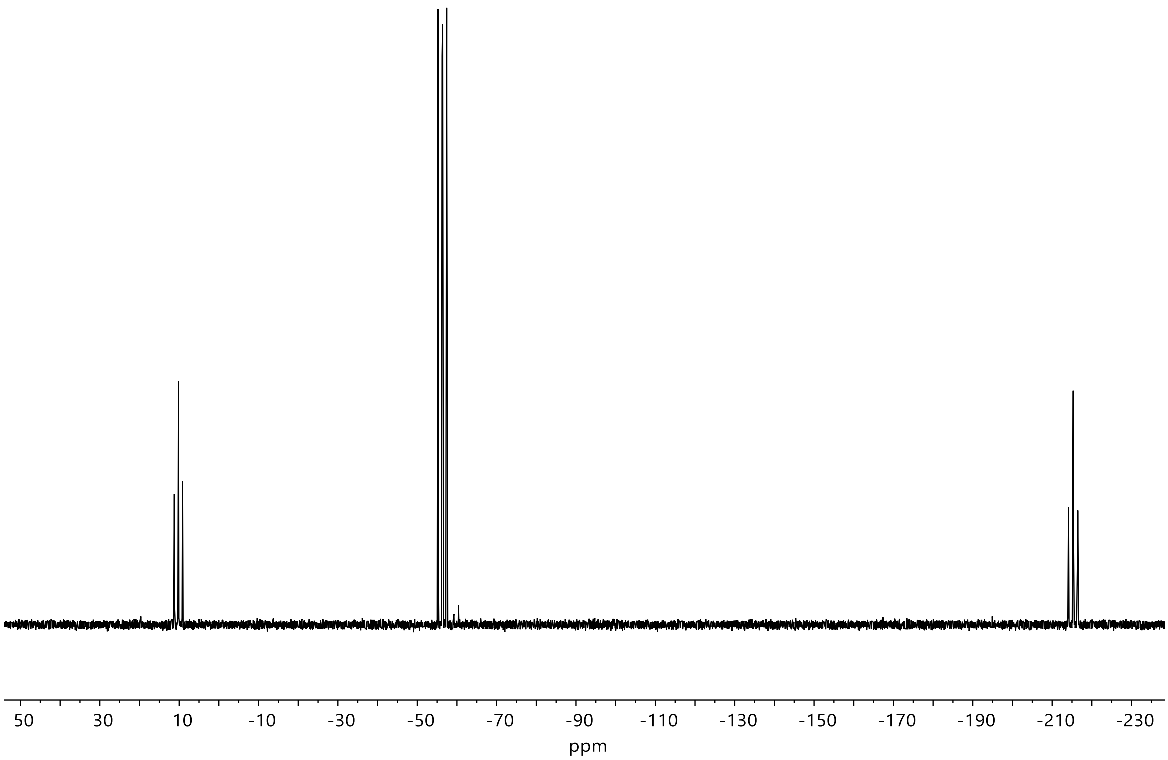

Fig. S4 $^{31}P\{^{1}H\}$ NMR spectrum of **1** at 162 MHz.

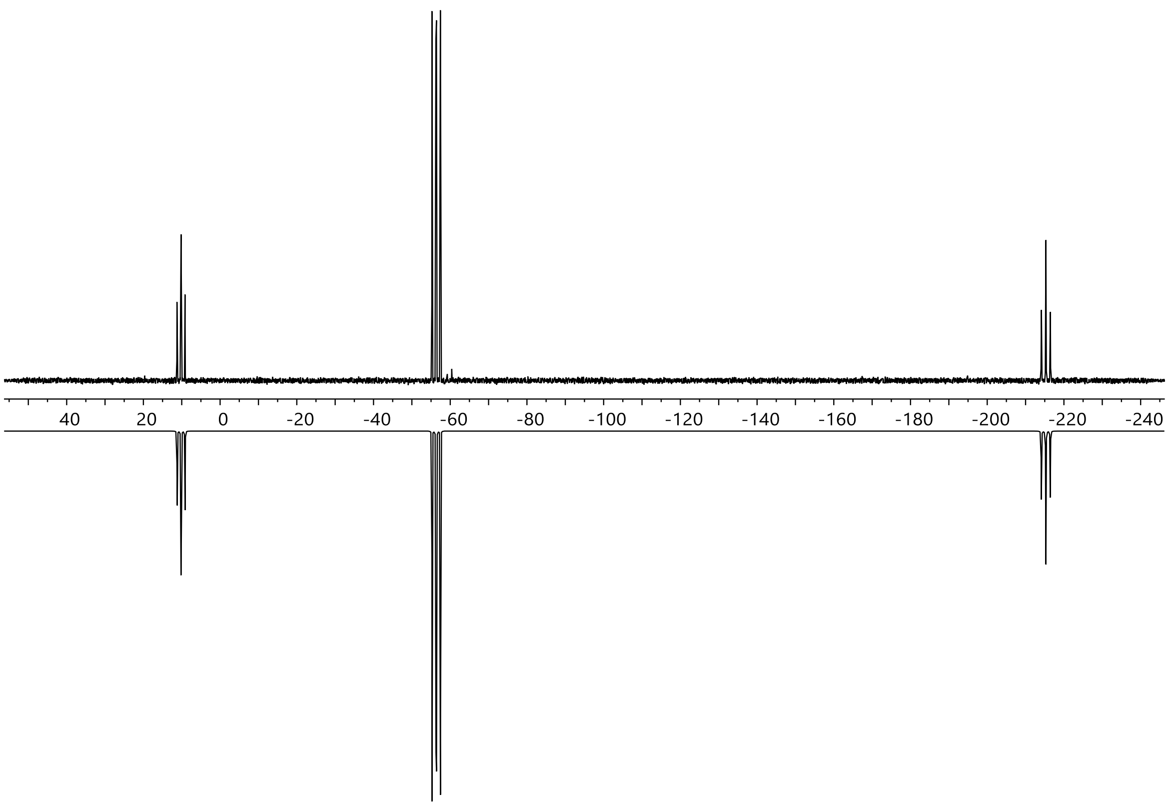

Fig. S5 Experimental (top) and simulated (bottom) $^{31}P\{^{1}H\}$ NMR spectrum of **1** at 162 MHz.

3.2. {*cyclo*-($P_4{}^tBu_3$)}$_2$ (2)

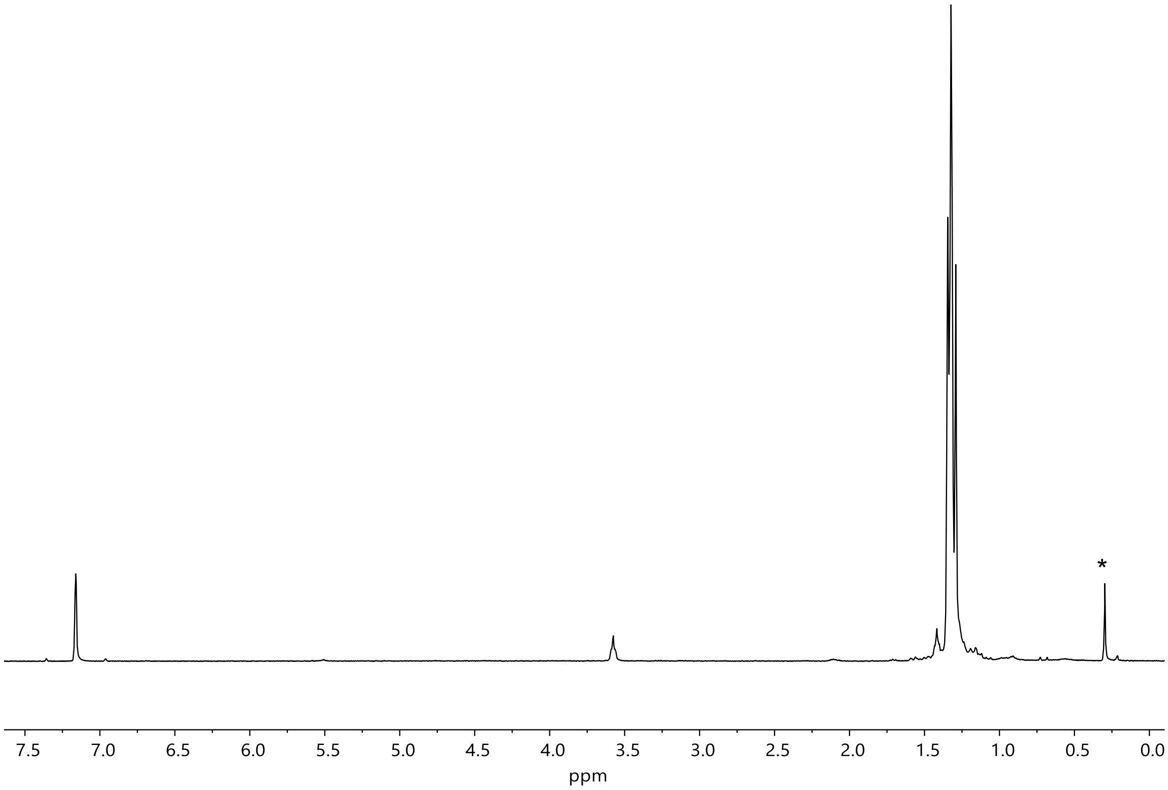

Fig. S6 ^{1}H NMR spectrum of **2**·2 THF at 400 MHz. * = silicon grease

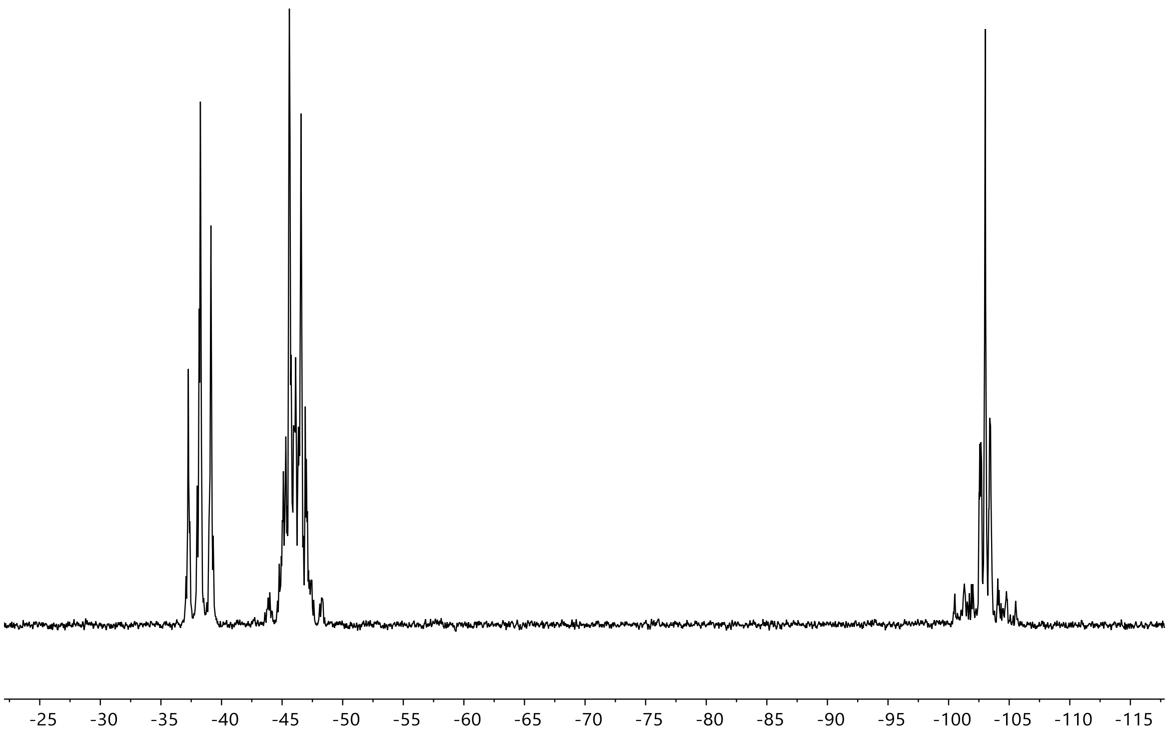

Fig. S7 ^{31}P{^{1}H} NMR spectrum of **2**·2 THF at 162 MHz (ns = 9567).

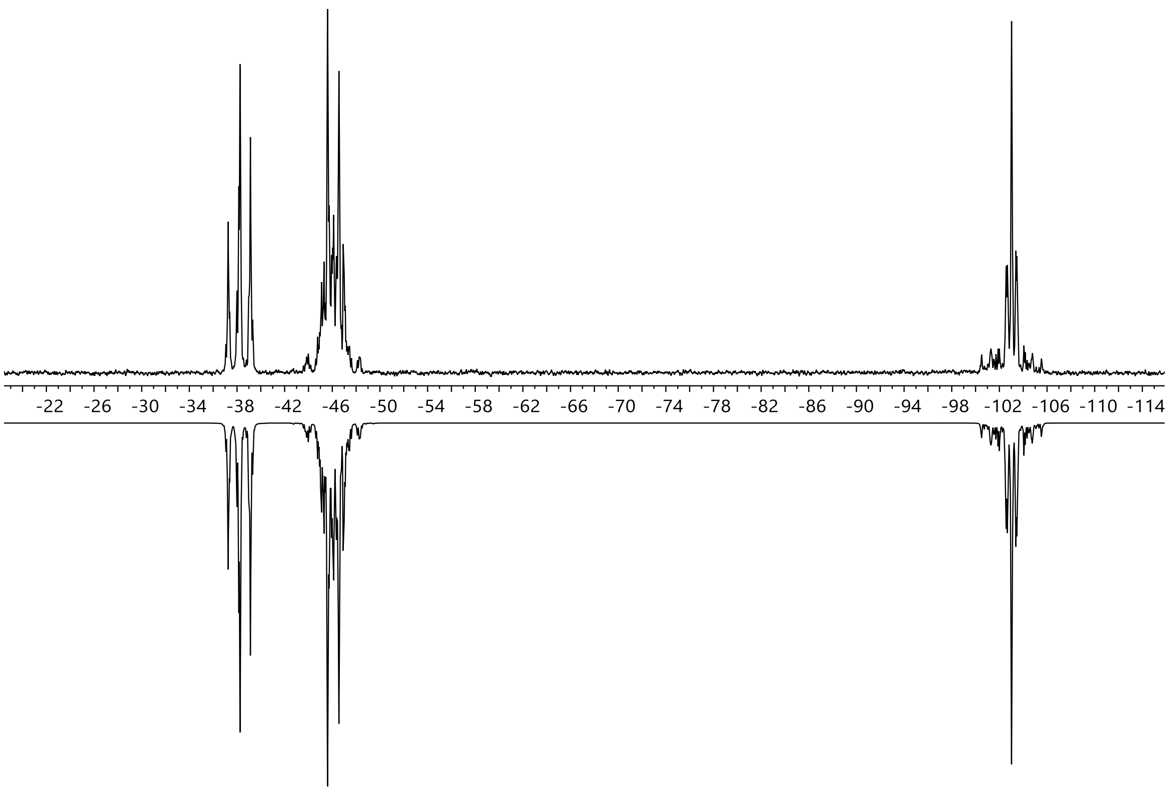

Fig. S8 Experimental (top) and simulated (bottom) $^{31}P\{^{1}H\}$ NMR spectrum of **2**·2 THF at 162 MHz.

3.3. {*cyclo*-($P_4{}^tBu_3$)}$_2$P^{t}Bu (3)

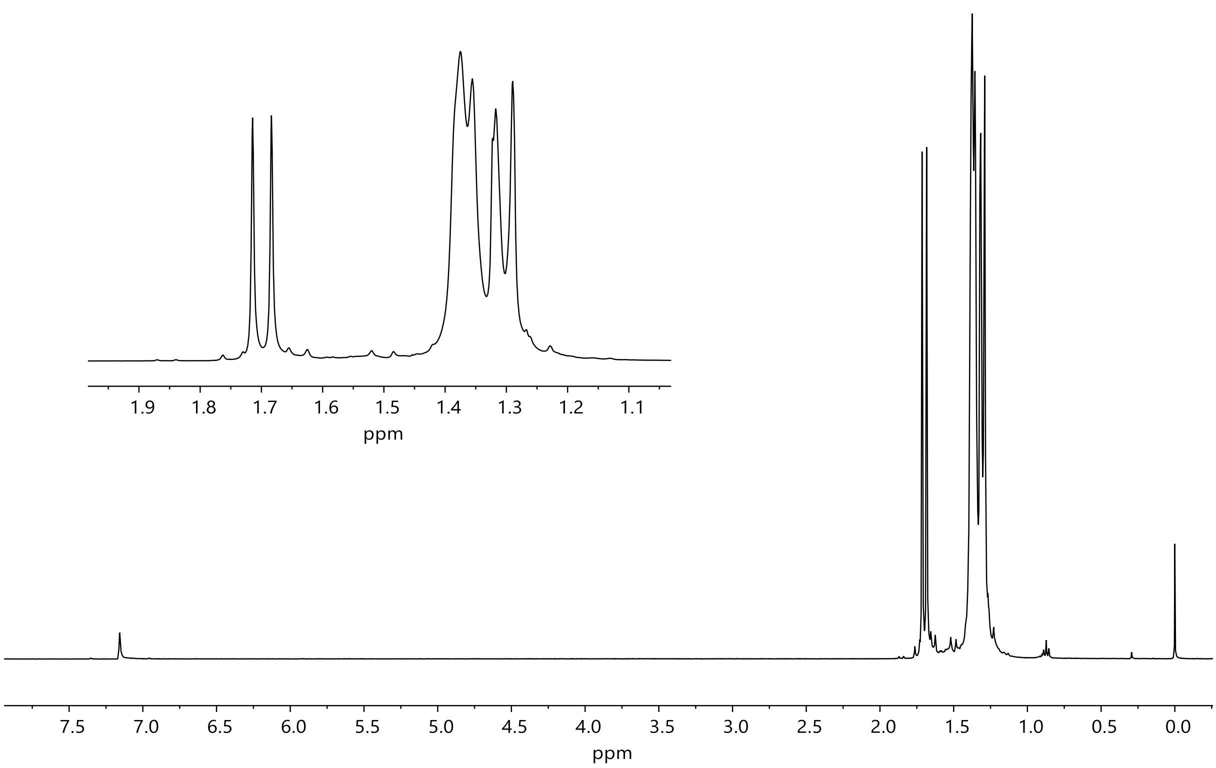

Fig. S9 ^{1}H NMR spectrum of **3** at 400 MHz.

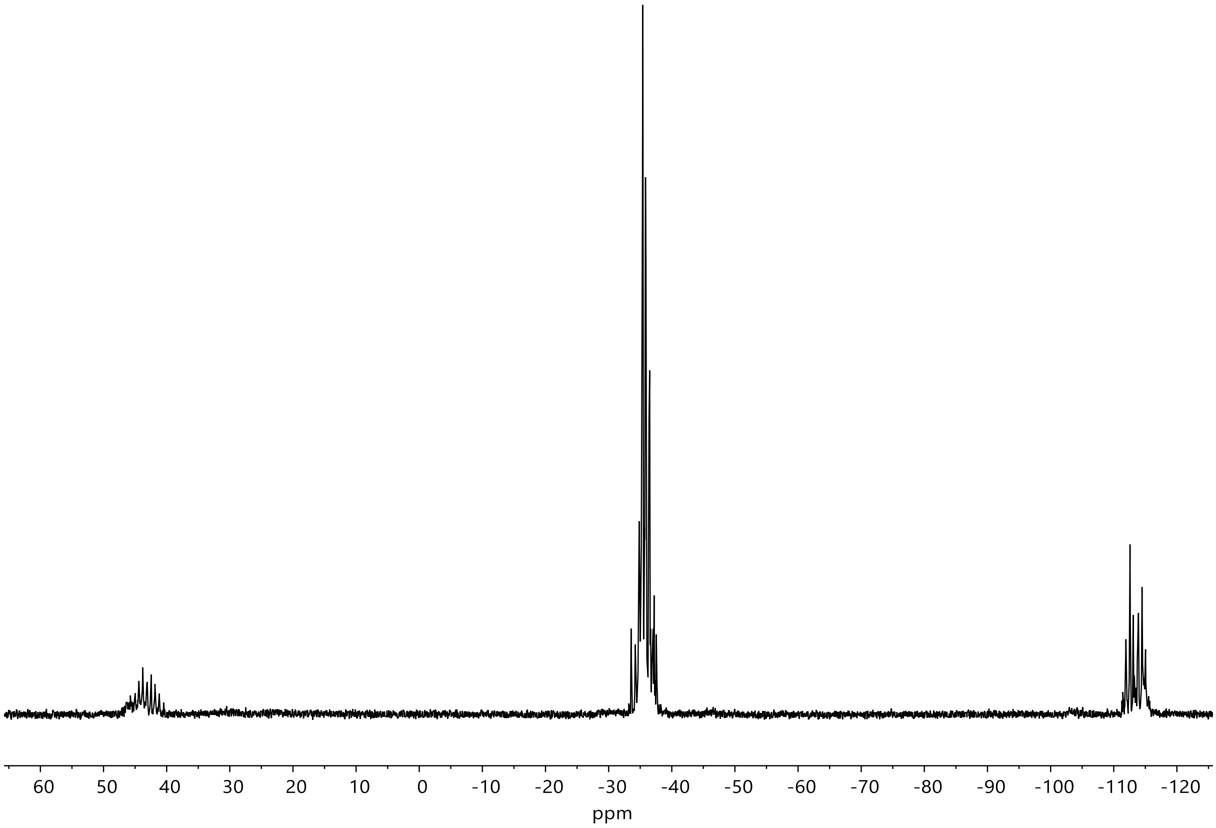

Fig. S10 $^{31}P\{^1H\}$ NMR spectrum of **3** at 162 MHz (ns = 7533).

3.4. {*cyclo*-($P_4{}^tBu_3$)}$_2$$CH_2$ (4)

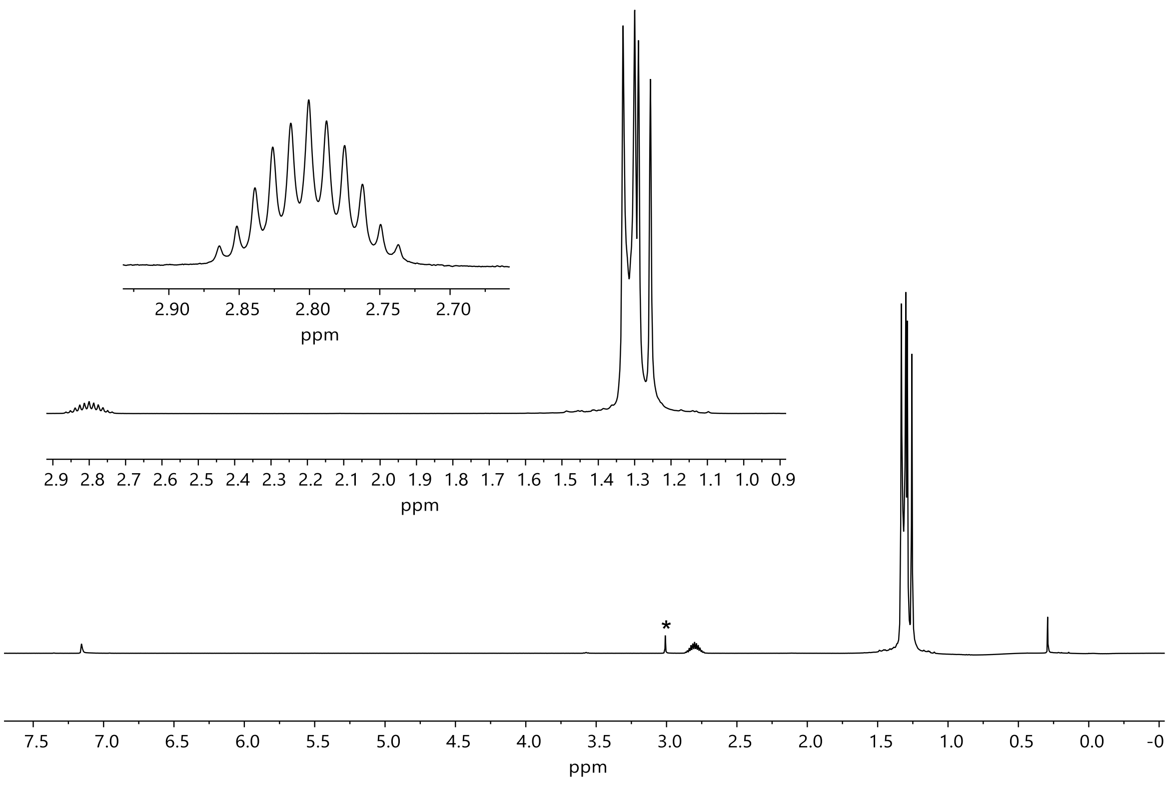

Fig. S11 ^1H NMR spectrum of **4** at 400 MHz. Residual methanol is marked with an asterisk.

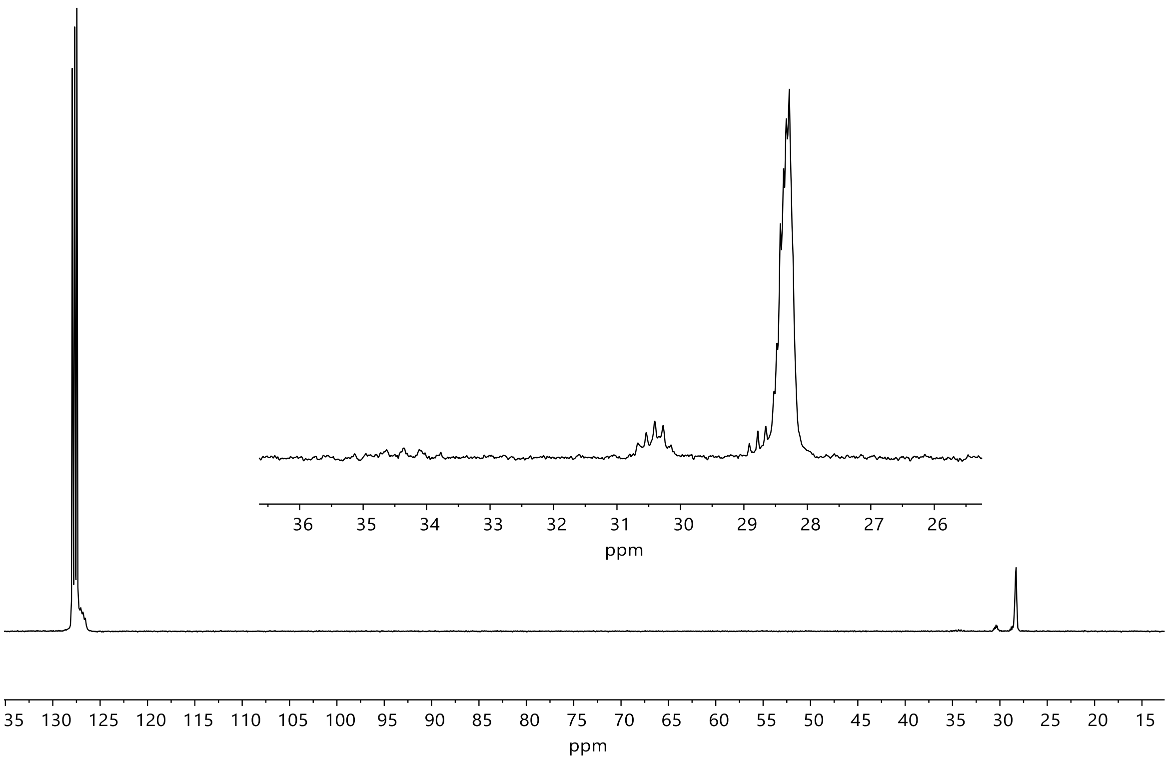

Fig. S12 $^{13}C\{^1H\}$ NMR spectrum of **4** at 101 MHz (ns = 4096).

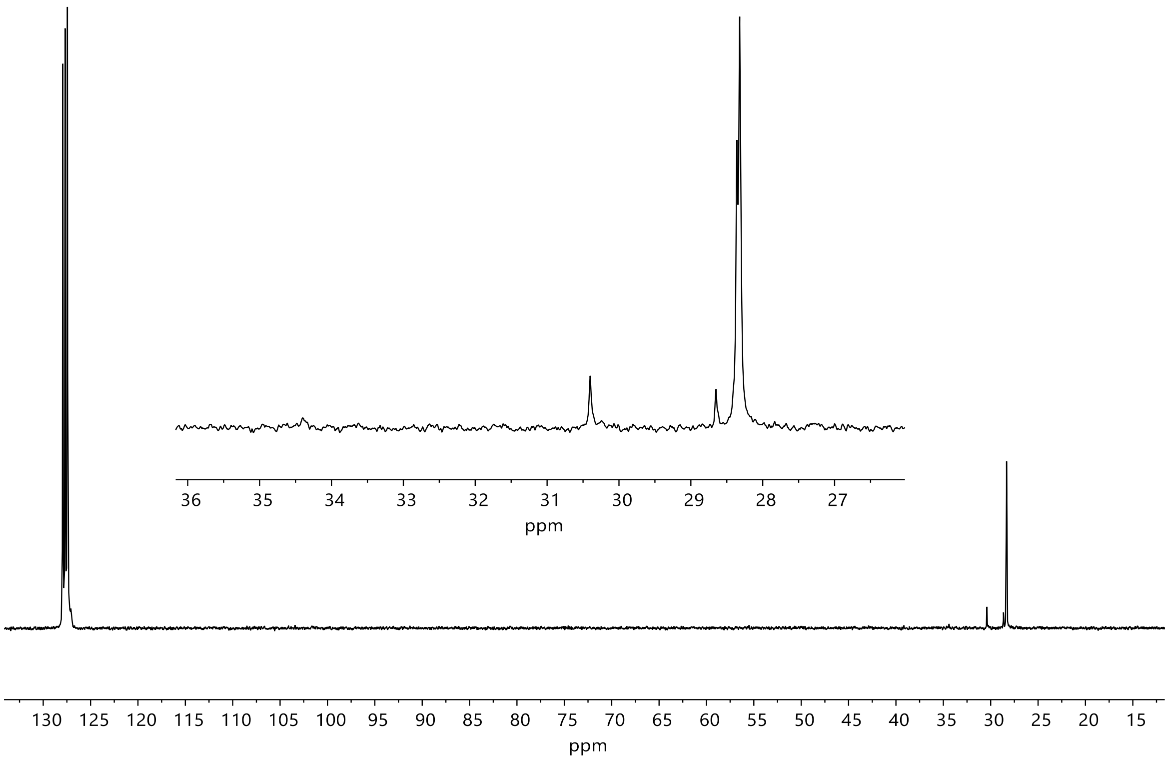

Fig. S13 $^{13}C\{^1H,^{31}P\}$ NMR spectrum of **4** at 101 MHz and 28 °C (ns = 8192).

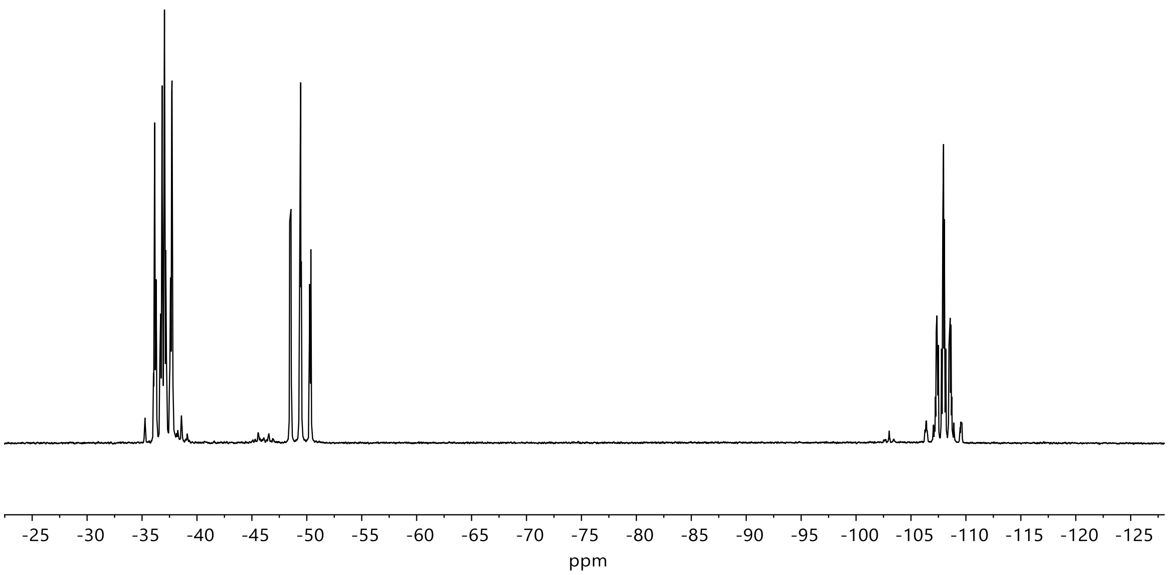

Fig. S14 $^{31}P\{^{1}H\}$ NMR spectrum of **4** at 162 MHz (ns = 10842).

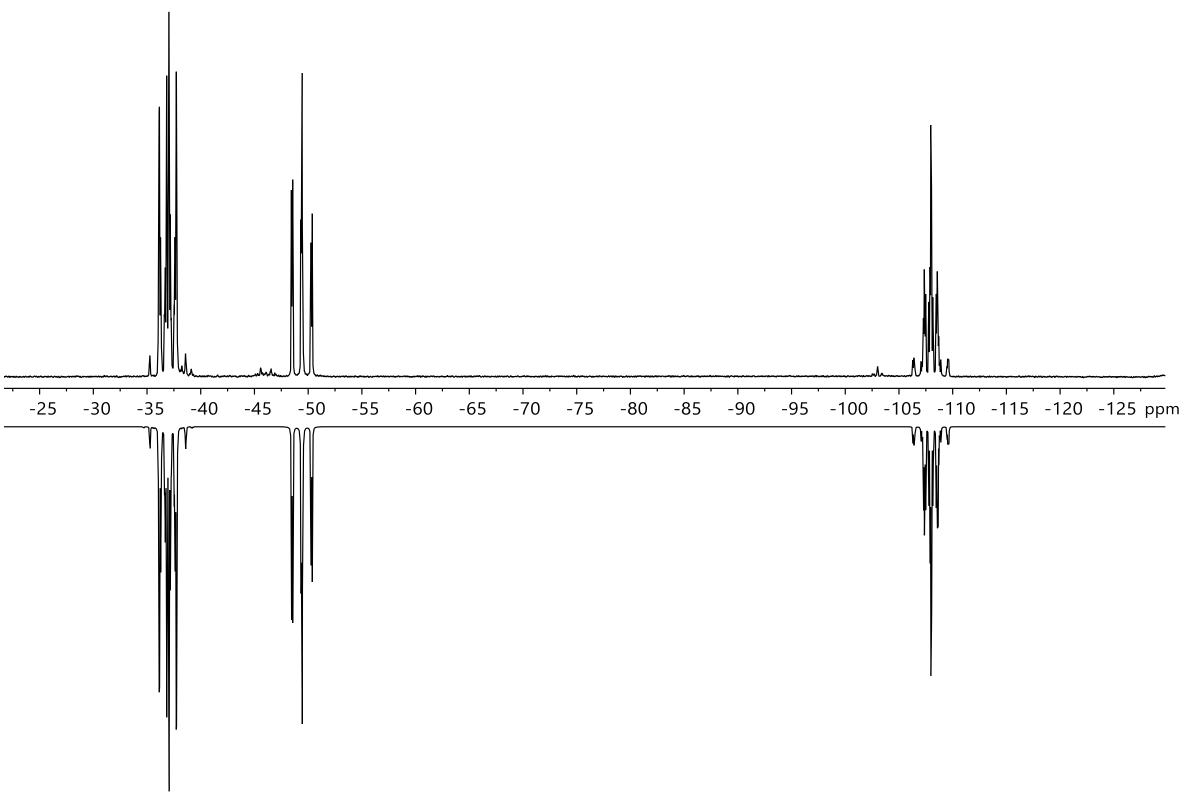

Fig. S15 Experimental (top) and simulated (bottom) $^{31}P\{^{1}H\}$ NMR spectrum of **4** at 162 MHz.

3.5. Bi{*cyclo*-($P_4{}^tBu_3$)}$_3$ (5)

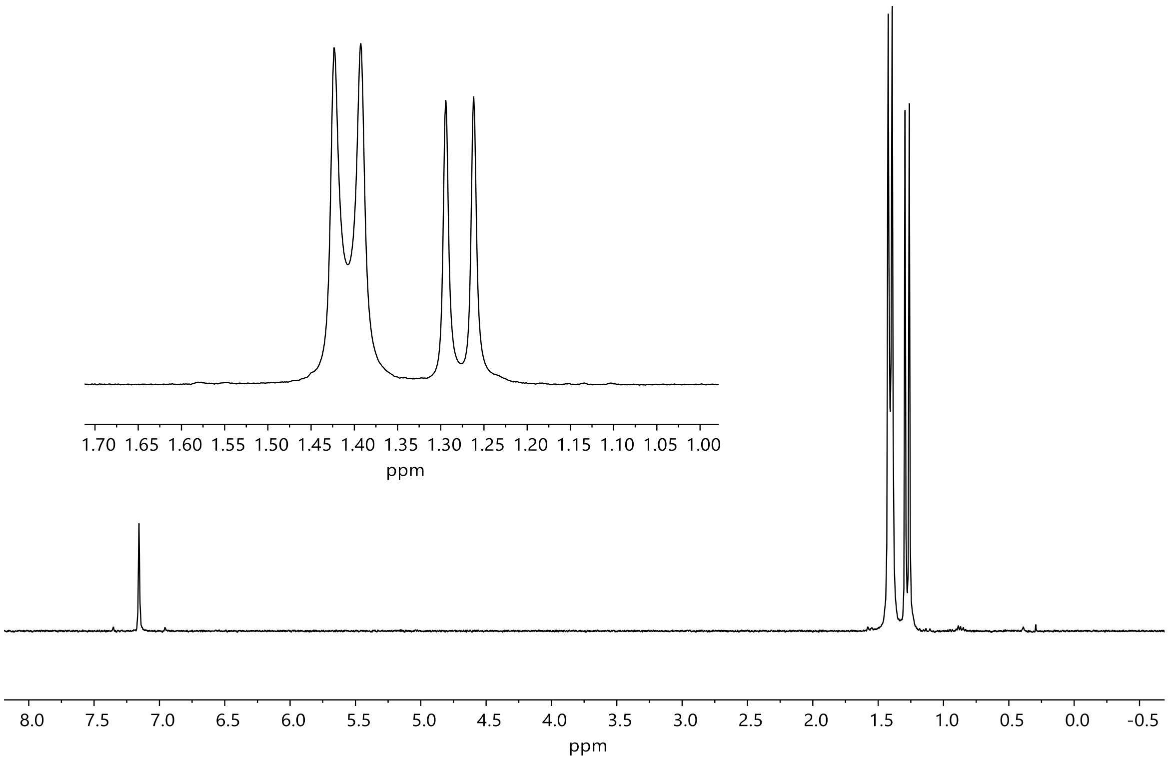

Fig. S16 ^{1}H NMR spectrum of **5** at 400 MHz.

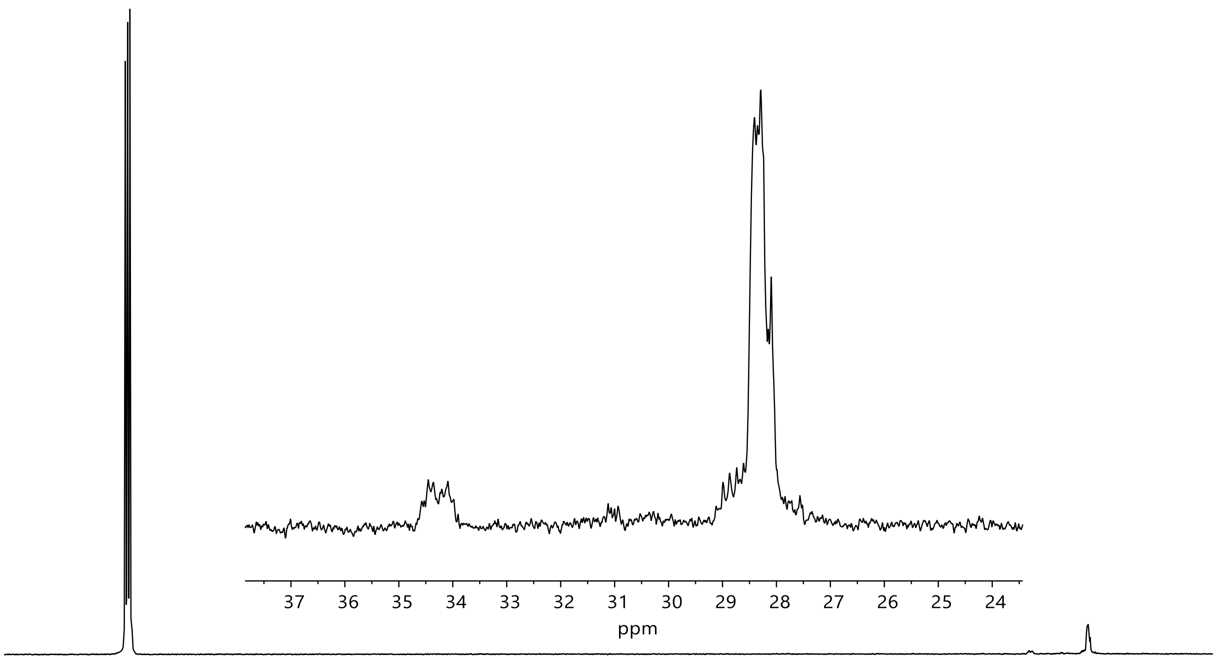

Fig. S17 $^{13}C\{^1H\}$ NMR spectrum of **5** at 101 MHz (ns = 4096).

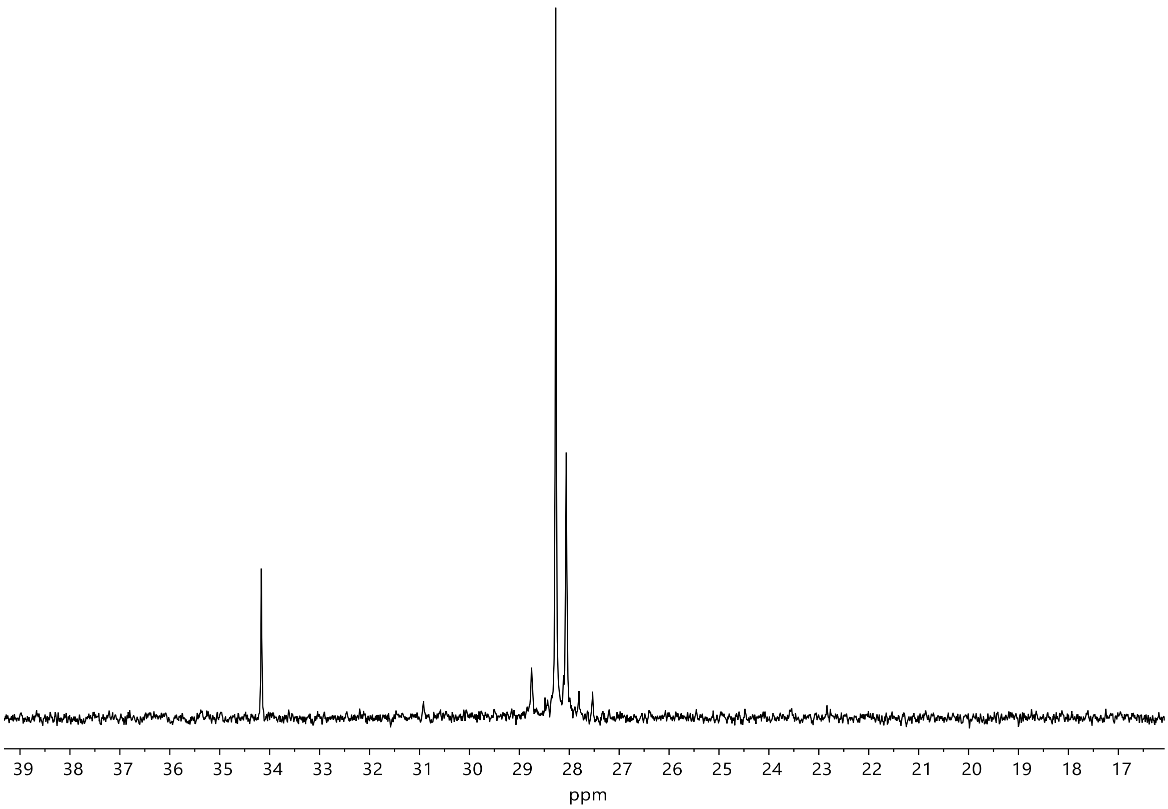

Fig. S18 $^{13}C\{^1H,^{31}P\}$ NMR spectrum of **5** at 101 MHz and 28 °C (ns = 10240).

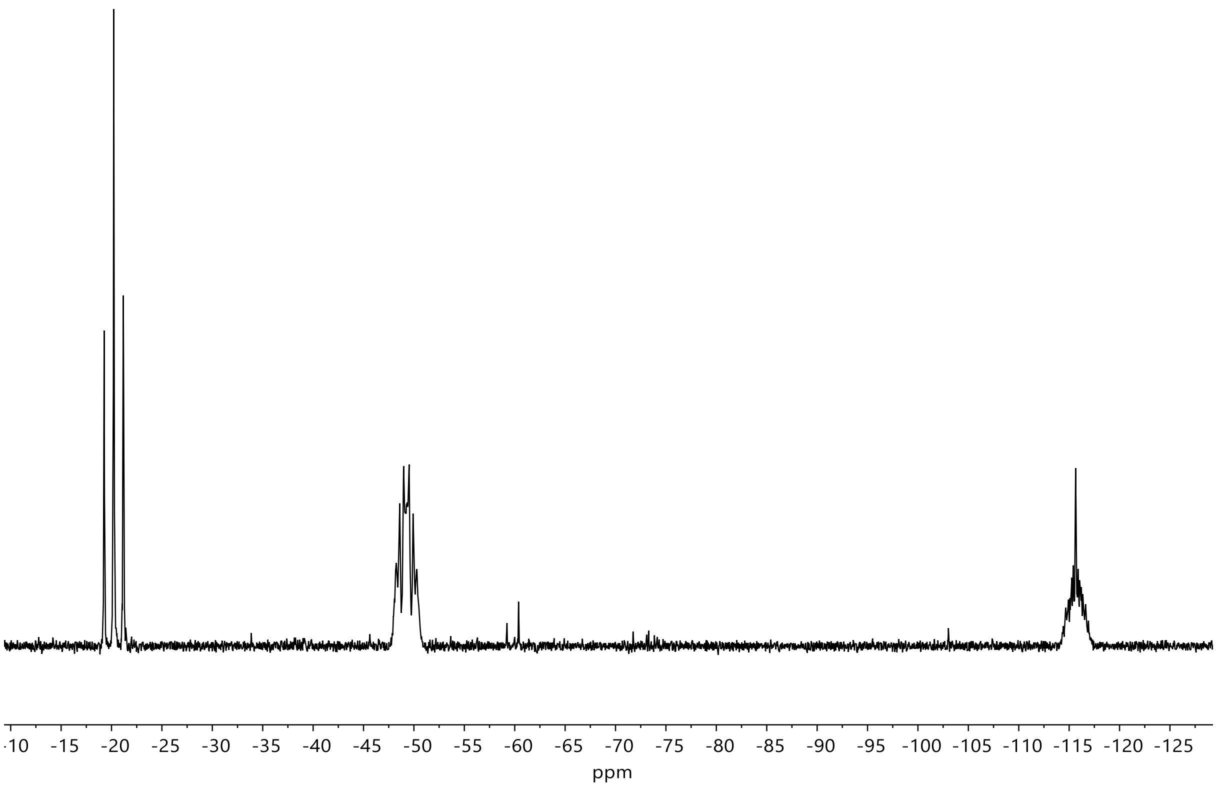

Fig. S19 $^{31}P\{^1H\}$ NMR spectrum of **5** at 162 MHz (ns = 10423).

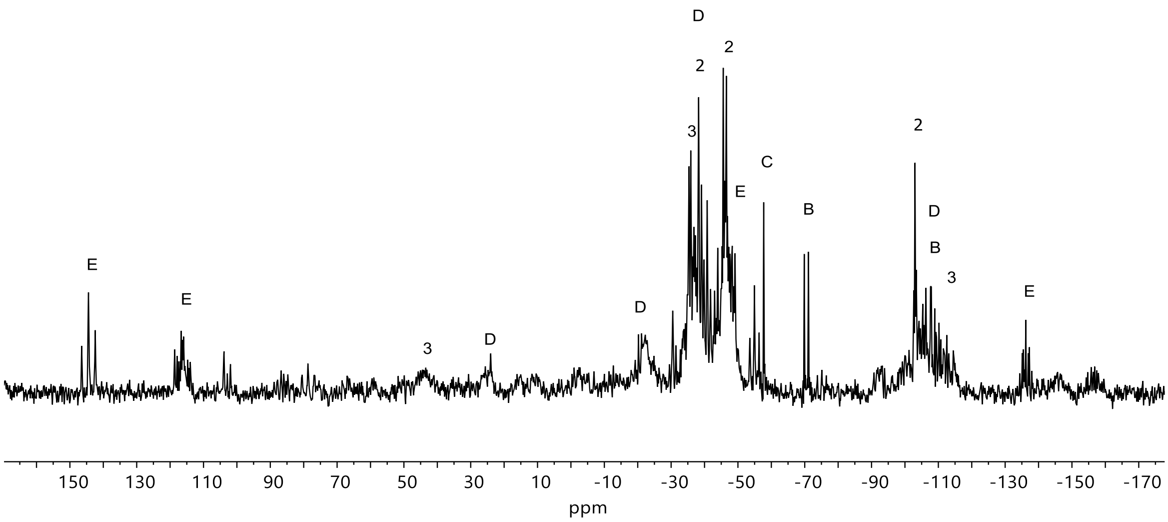

Fig. S20 $^{31}P\{^1H\}$ NMR spectrum at 162 MHz of a solution of **5** in C_6D_6 after one hour exposure to sunlight. **2**,[2] **3**,[3] **B** = *cyclo*-$(P^tBu)_3$,[4] **C** = *cyclo*-$(P^tBu)_4$,[5] **D** = $\{$*cyclo*-$(P_4{}^tBu_3)^tBu\}_2$,[3] **E** = $P_6{}^tBu_4$[6] (ns = 32768, lb = 15 Hz). The region below −100 ppm displays strong overlap of different signals. $P_7{}^tBu_5$ is also observed[7] but not assigned as not all of its resonances are visible due to the low quality of the spectrum.

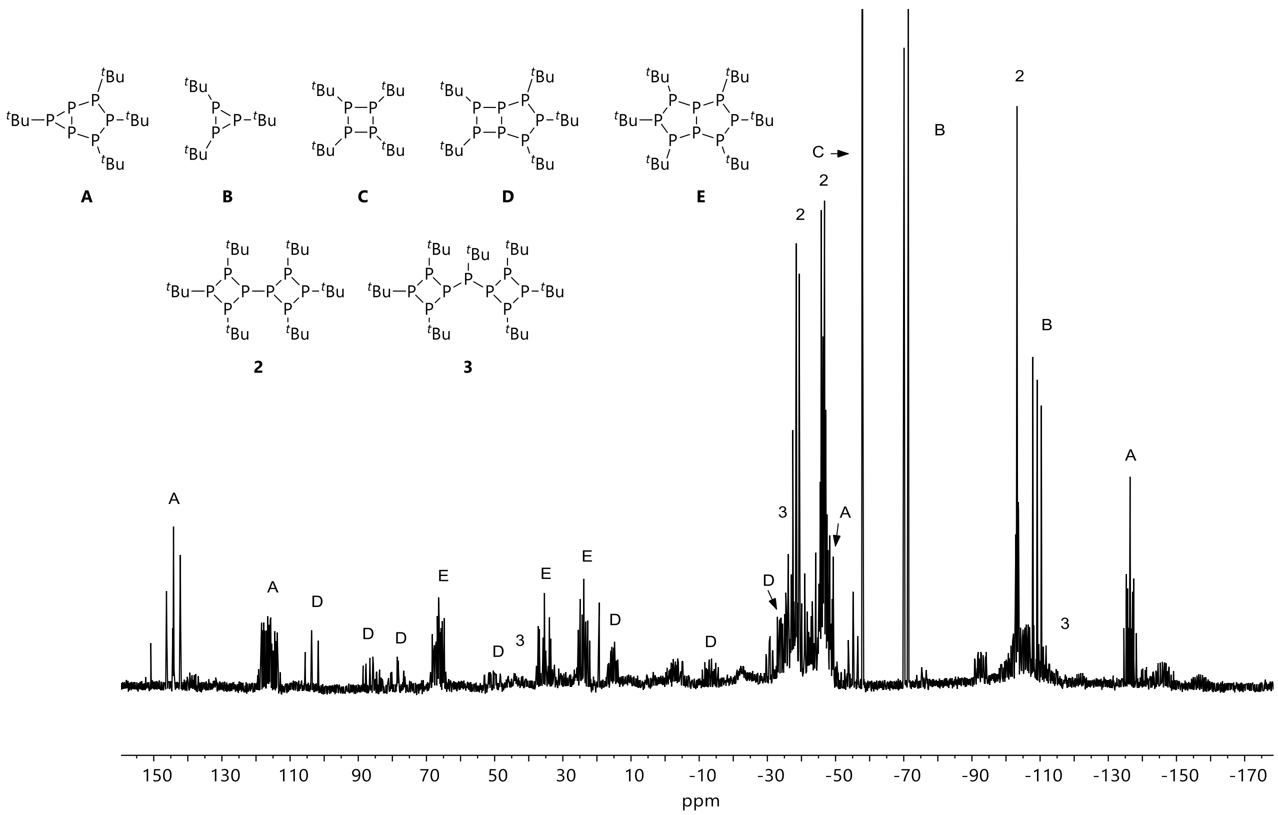

Fig. S21 $^{31}P\{^{1}H\}$ NMR spectrum at 162 MHz of a solution of **2**·2 THF in C_6D_6 exposed to the sunlight for 5 h. **A**,[6] **B**,[4] **C**,[5] **D**,[7] **E**,[8] **2**,[2] and **3**[3] are literature known.

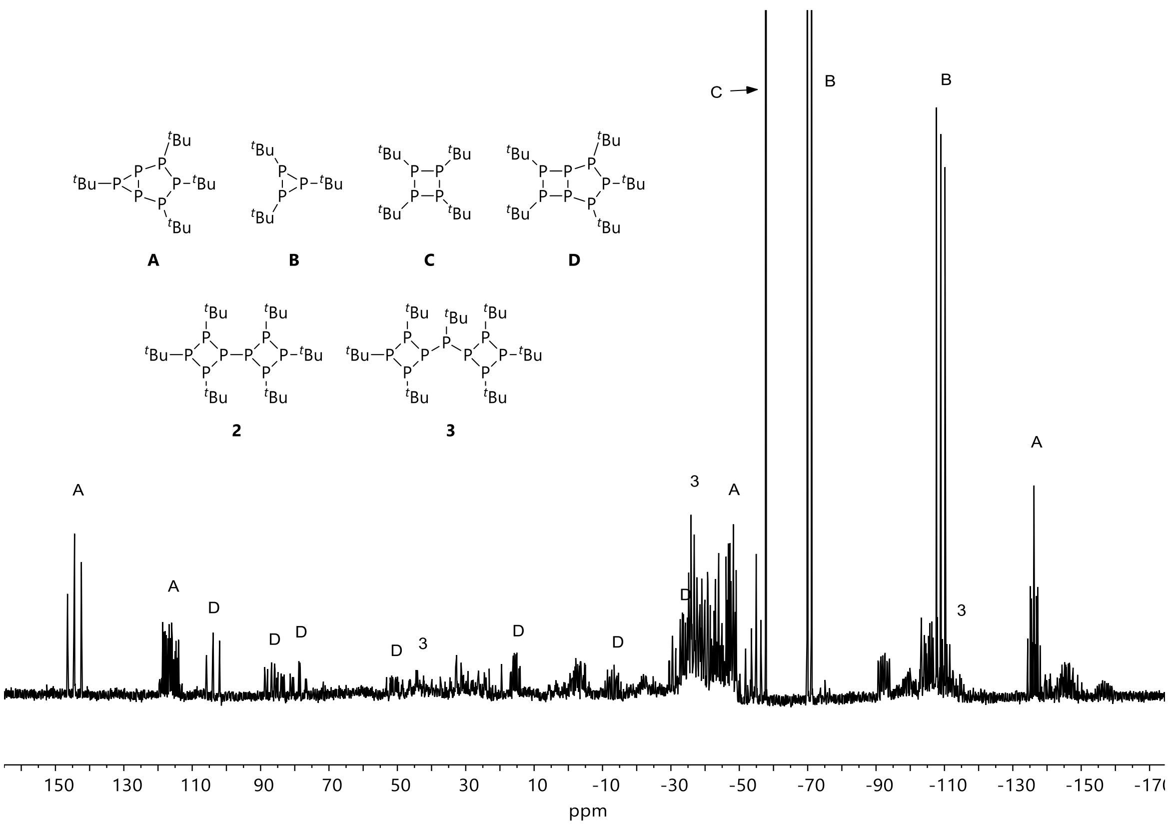

Fig. S22 $^{31}P\{^{1}H\}$ NMR spectrum at 162 MHz of a solution of **3** in C_6D_6 exposed to the sunlight for 5 h. **A**,[6] **B**,[4] **C**,[5] **D**,[7] **2**,[2] and **3**[3] are literature known.

3.6. Sb{*cyclo*-($P_4{}^tBu_3$)}$_3$ (6)

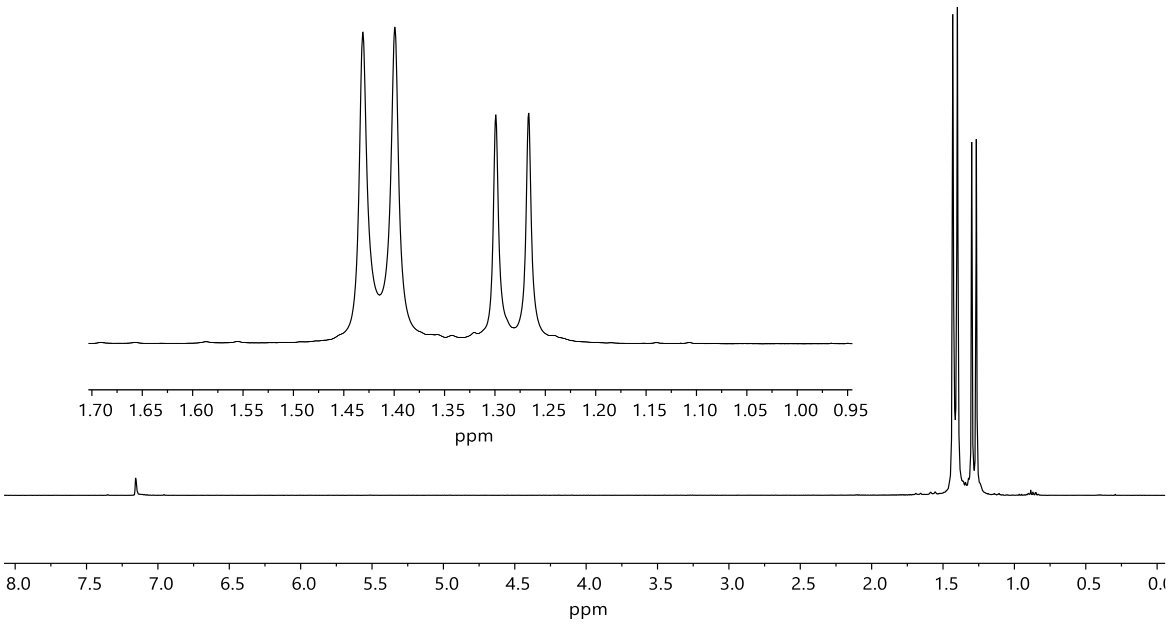

Fig. S23 ^{1}H NMR spectrum of **6** at 400 MHz.

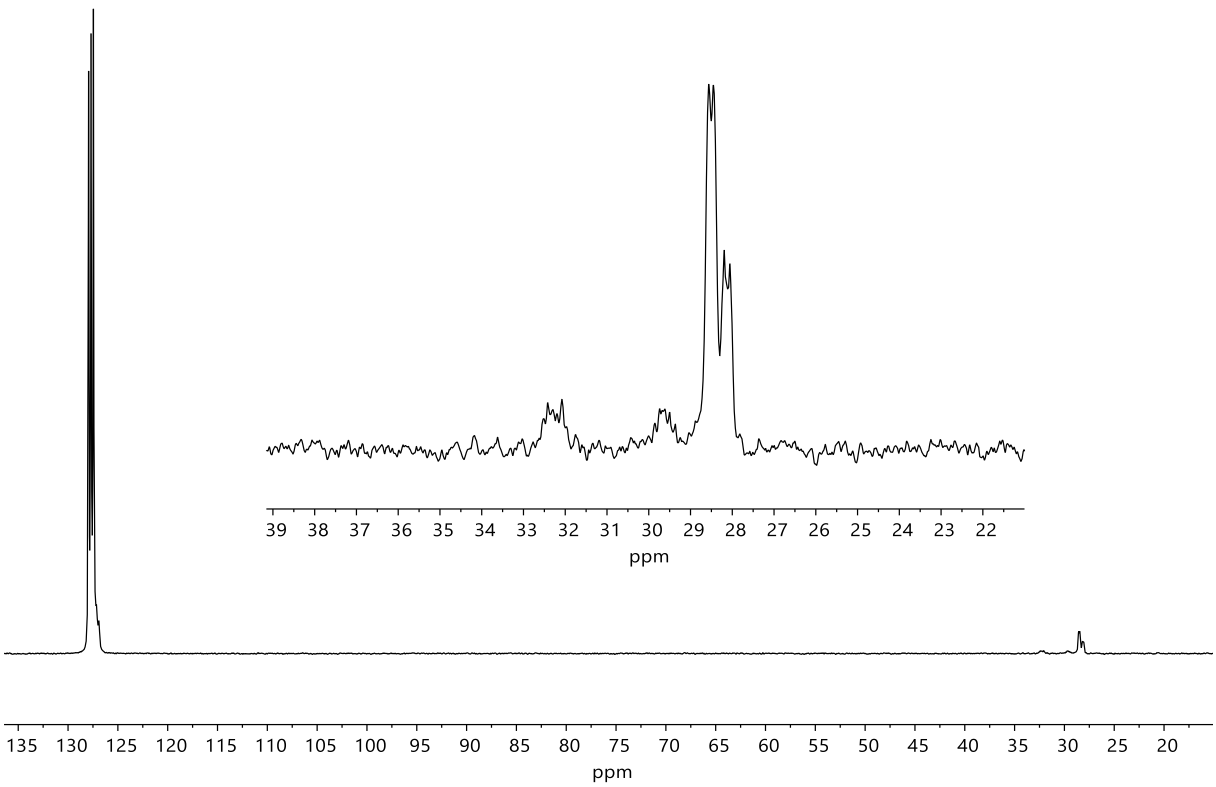

Fig. S24 $^{13}C\{^1H\}$ NMR spectrum of **6** at 101 MHz (ns = 2044).

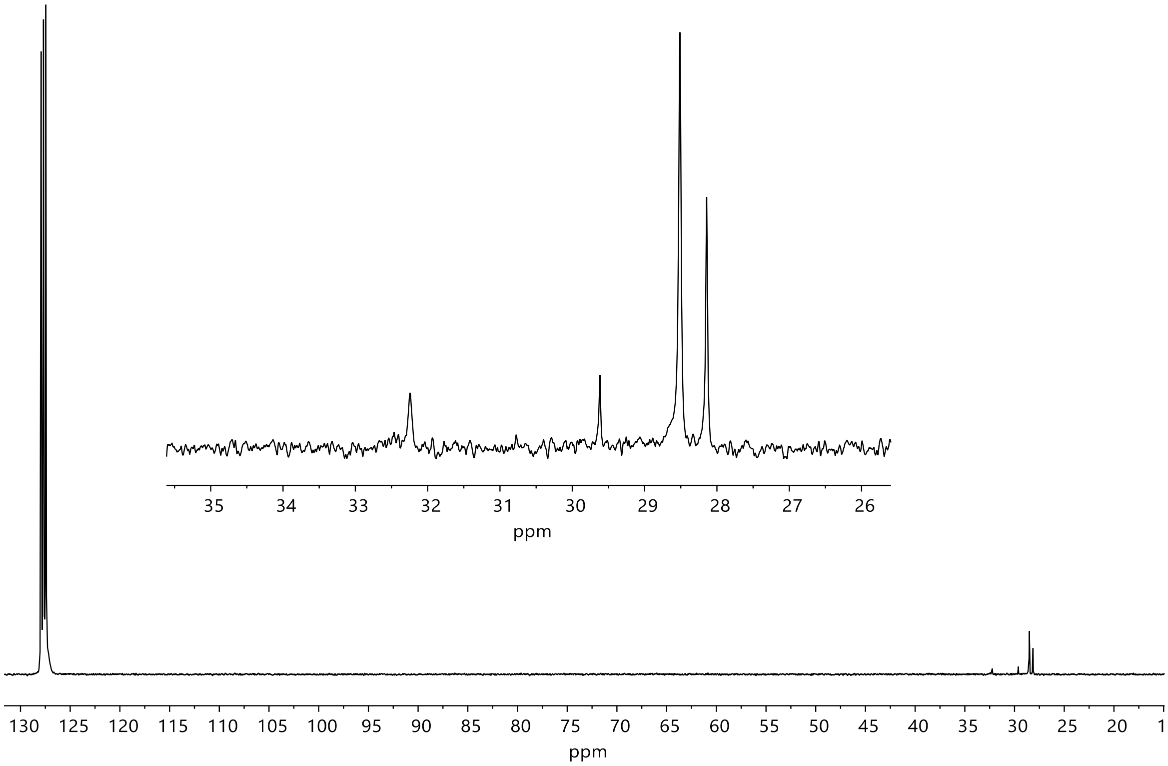

Fig. S25 $^{13}C\{^1H,^{31}P\}$ NMR spectrum of **6** at 101 MHz and 28 °C (ns = 8192).

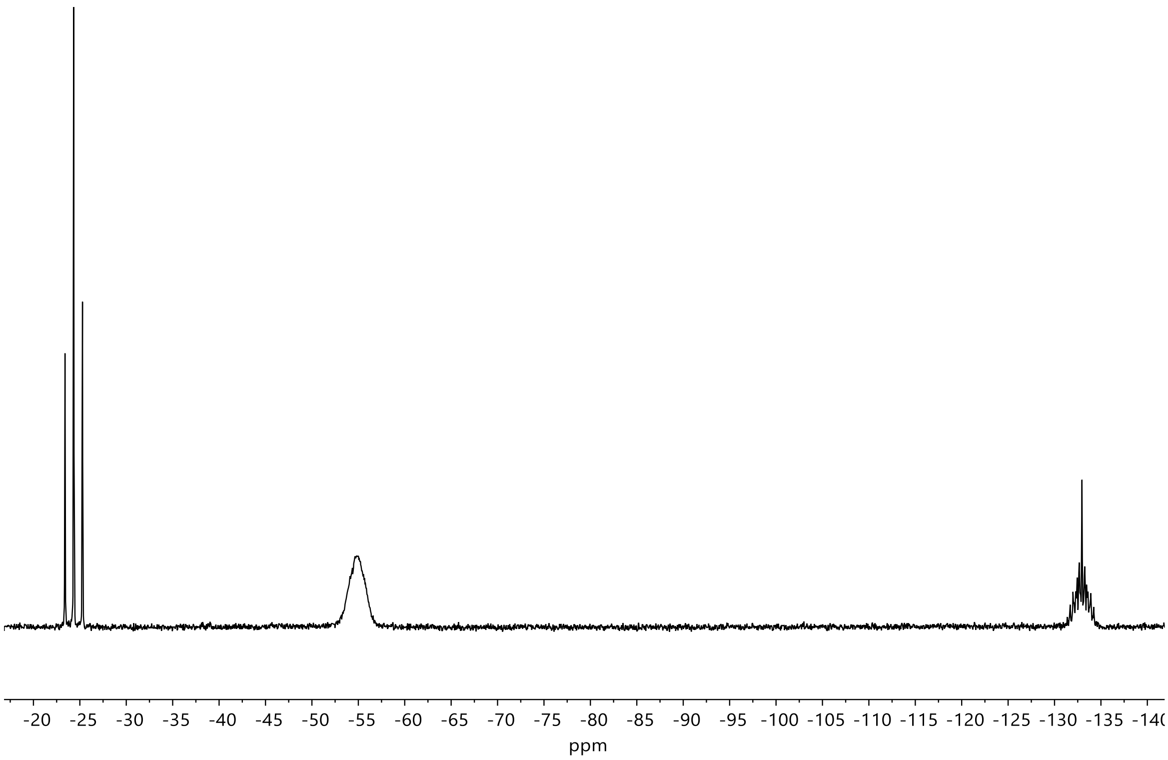

Fig. S26 $^{31}P\{^1H\}$ NMR spectrum of **6** at 162 MHz (ns = 1426).

3.7. As{*cyclo*-($P_4{}^tBu_3$)}$_3$ (7)

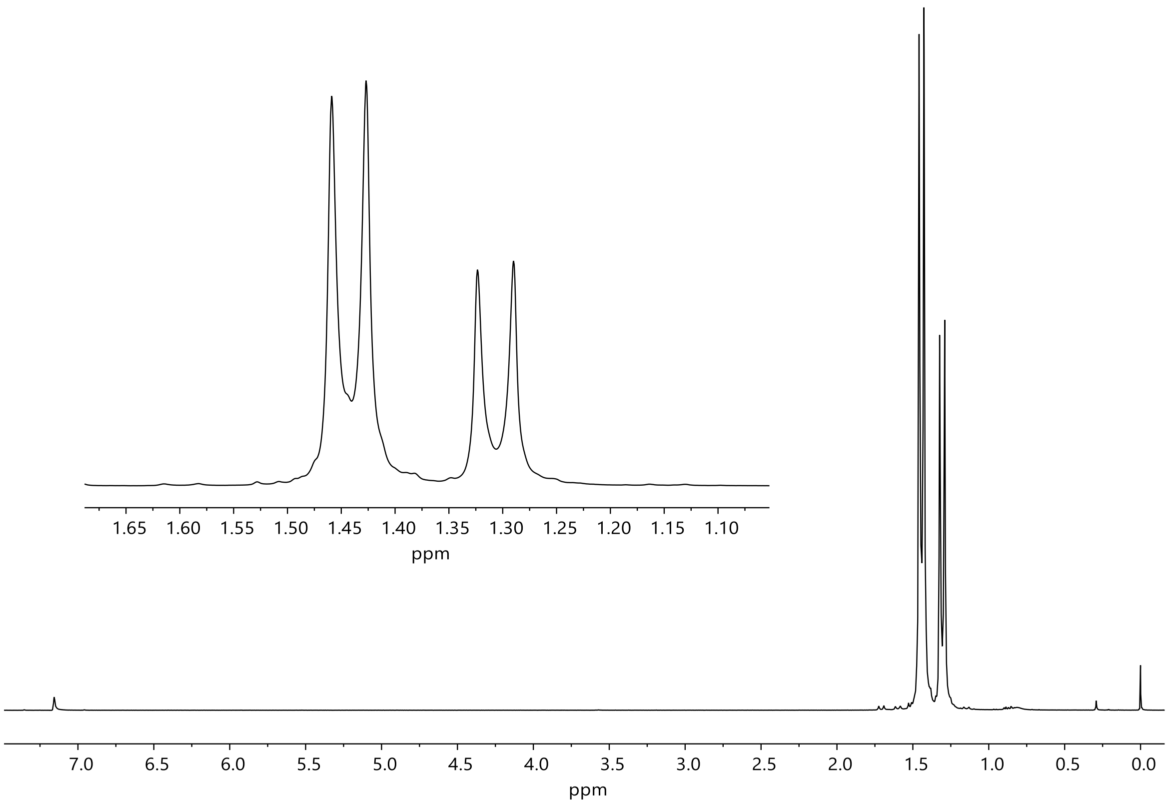

Fig. S27 ^{1}H NMR spectrum of **7** at 400 MHz.

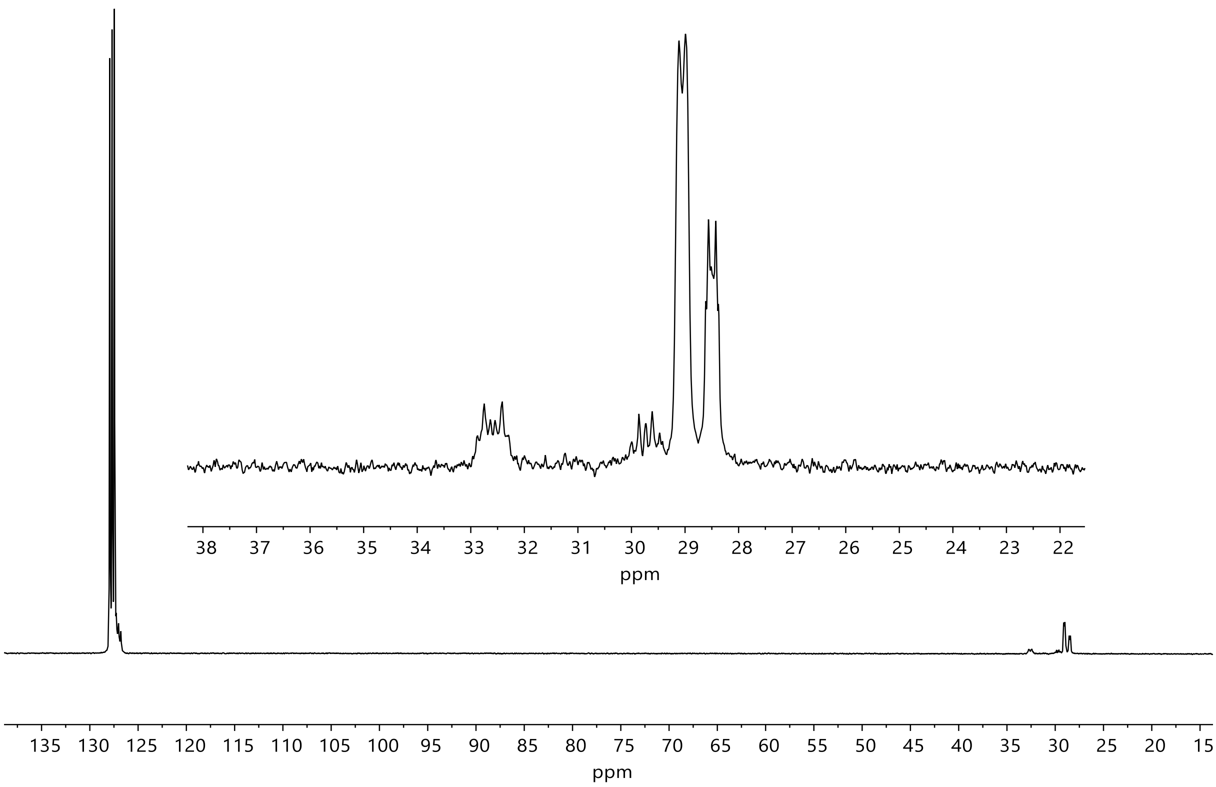

Fig. S28 ^{13}C{^{1}H} NMR spectrum of **7** at 101 MHz (ns = 4584).

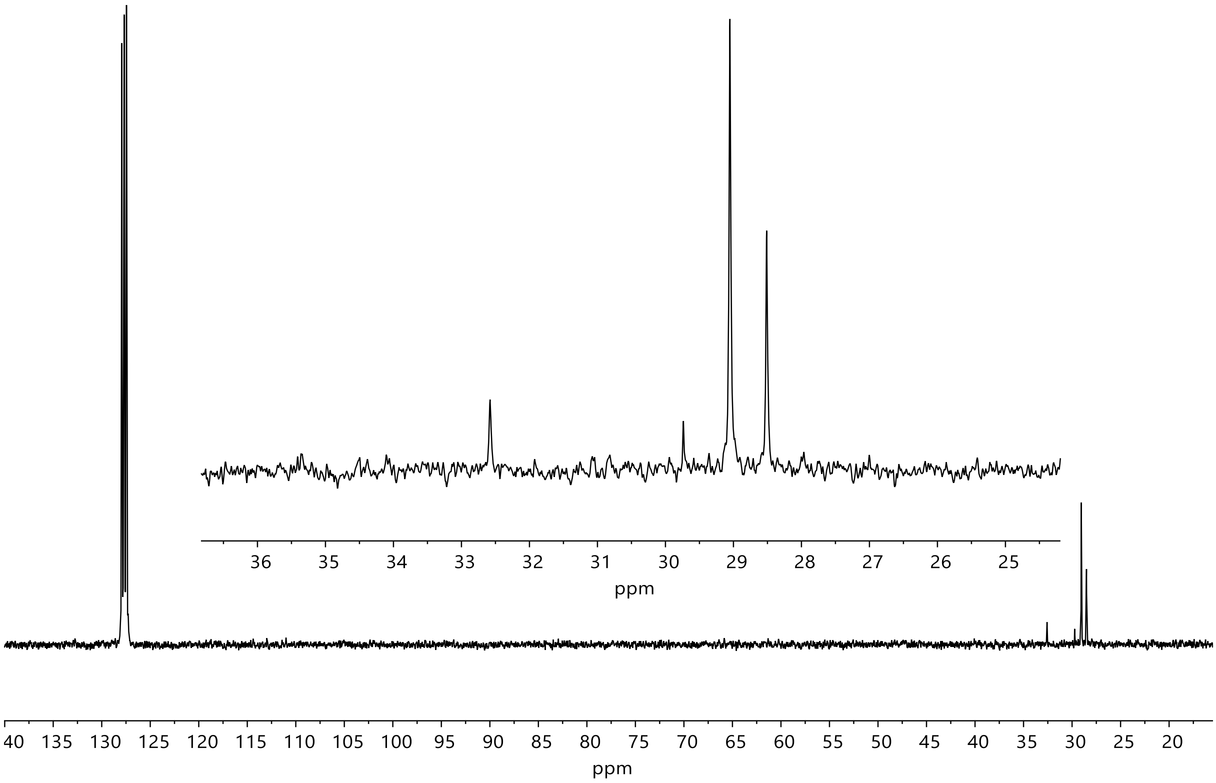

Fig. S29 $^{13}C\{^{1}H,^{31}P\}$ NMR spectrum of **7** at 101 MHz and 28 °C (ns = 4785).

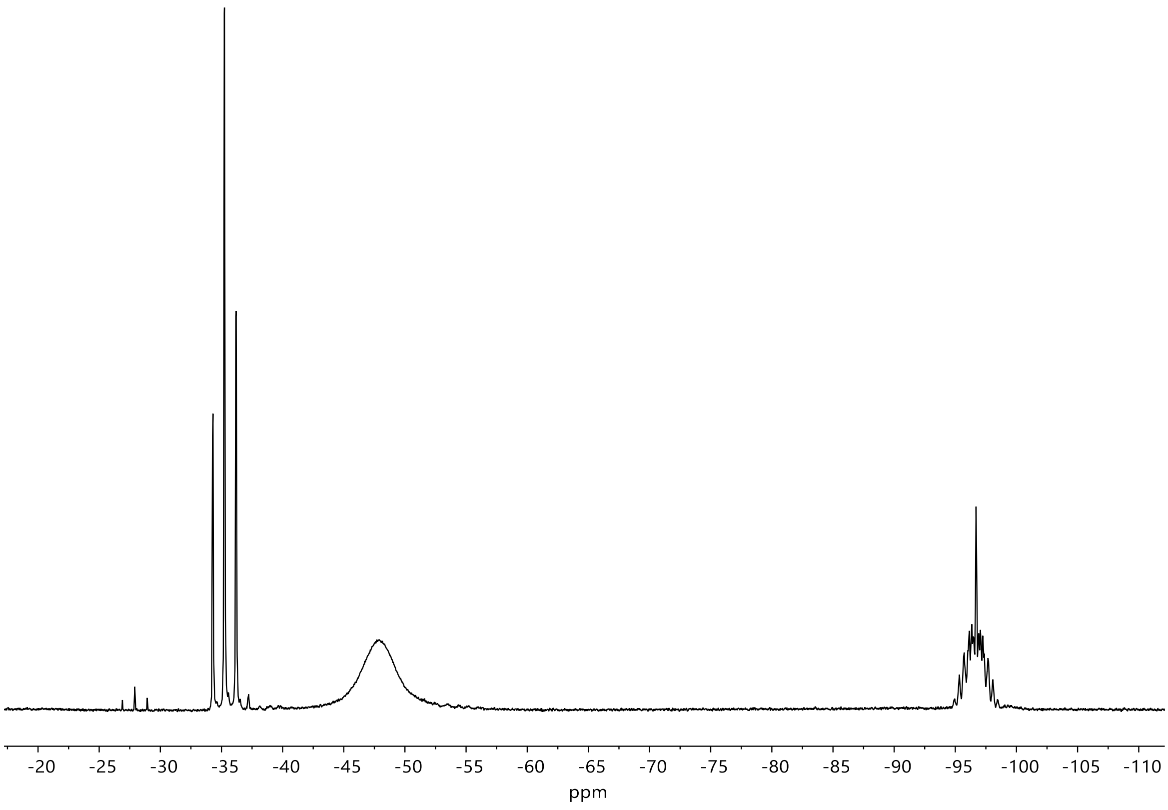

Fig. S30 $^{31}P\{^{1}H\}$ NMR spectrum of **7** at 162 MHz (ns = 8433).

3.8. As{*cyclo*-($P_4{}^tBu_3$)}$_2$Cl (8)

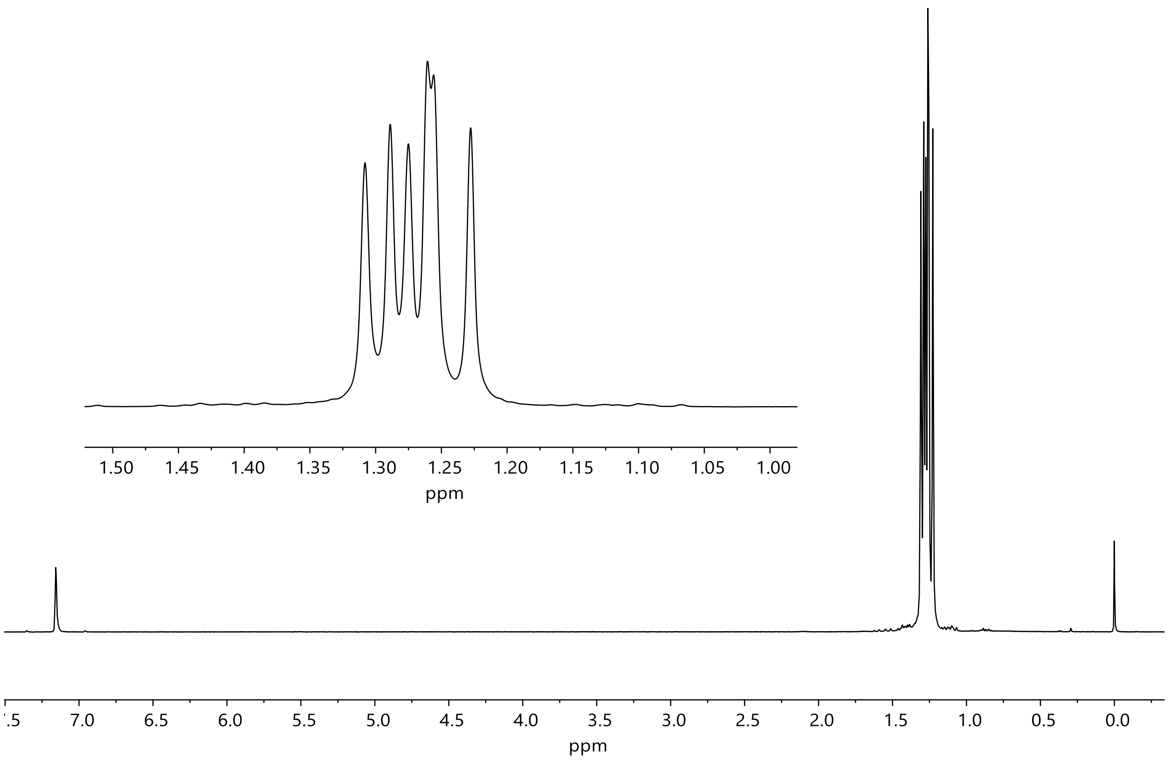

Fig. S31 ^{1}H NMR spectrum of **8** at 400 MHz.

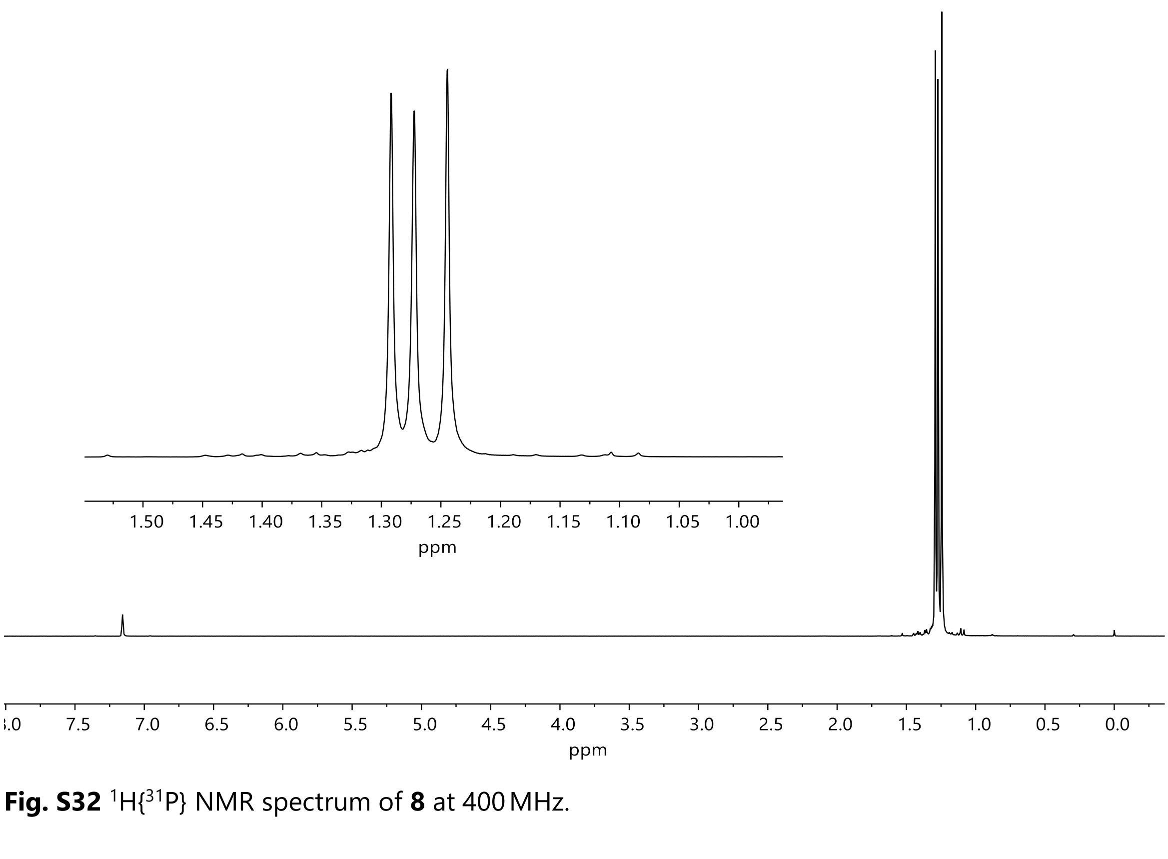

Fig. S32 ^{1}H{^{31}P} NMR spectrum of **8** at 400 MHz.

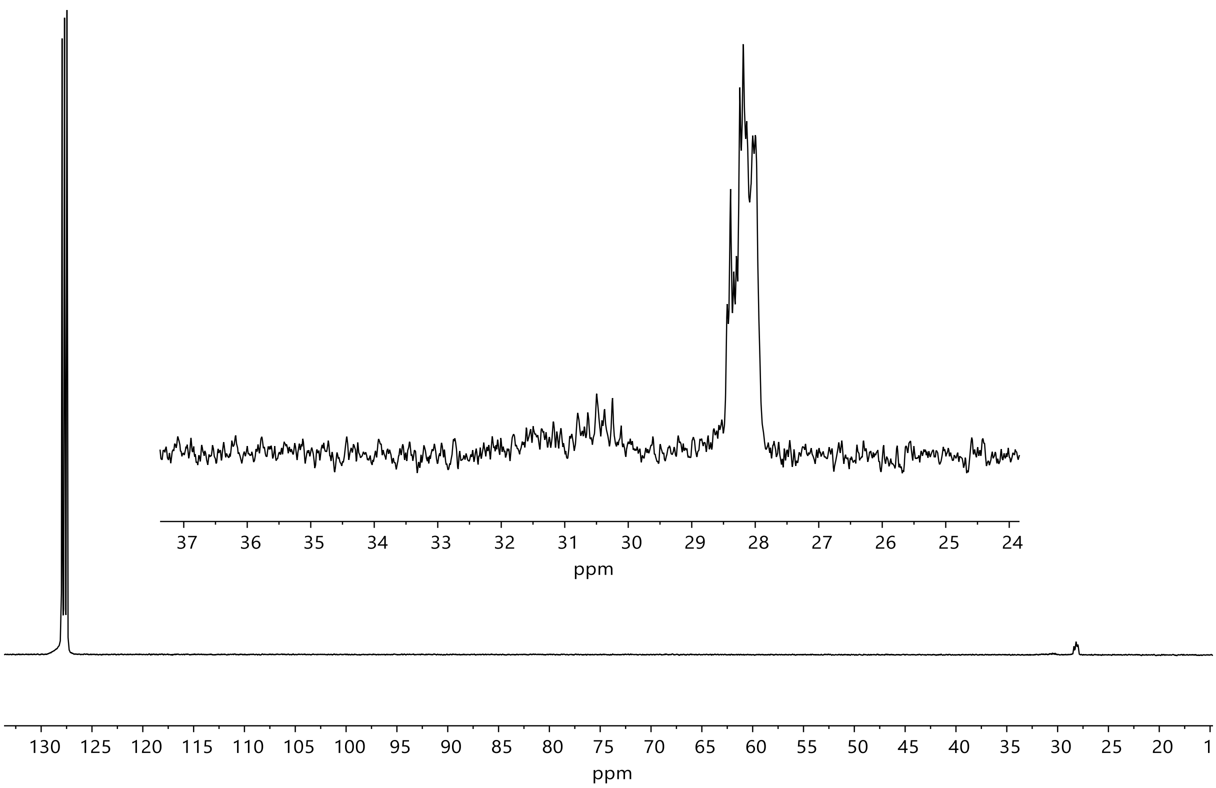

Fig. S33 $^{13}C\{^{1}H\}$ NMR spectrum of **8** at 101 MHz (ns = 2772).

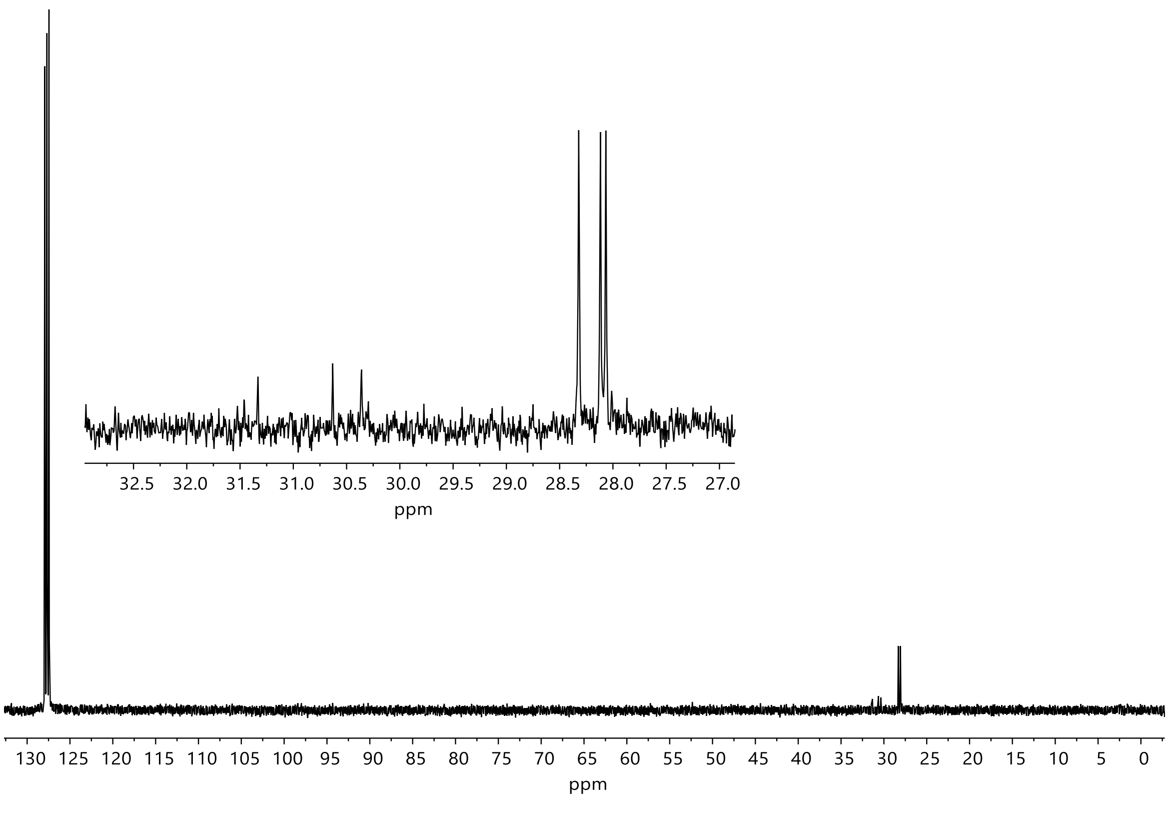

Fig. S34 $^{13}C\{^{1}H,^{31}P\}$ NMR spectrum of **8** at 101 MHz and 28 °C (ns = 13734; lb = 0.5 Hz).

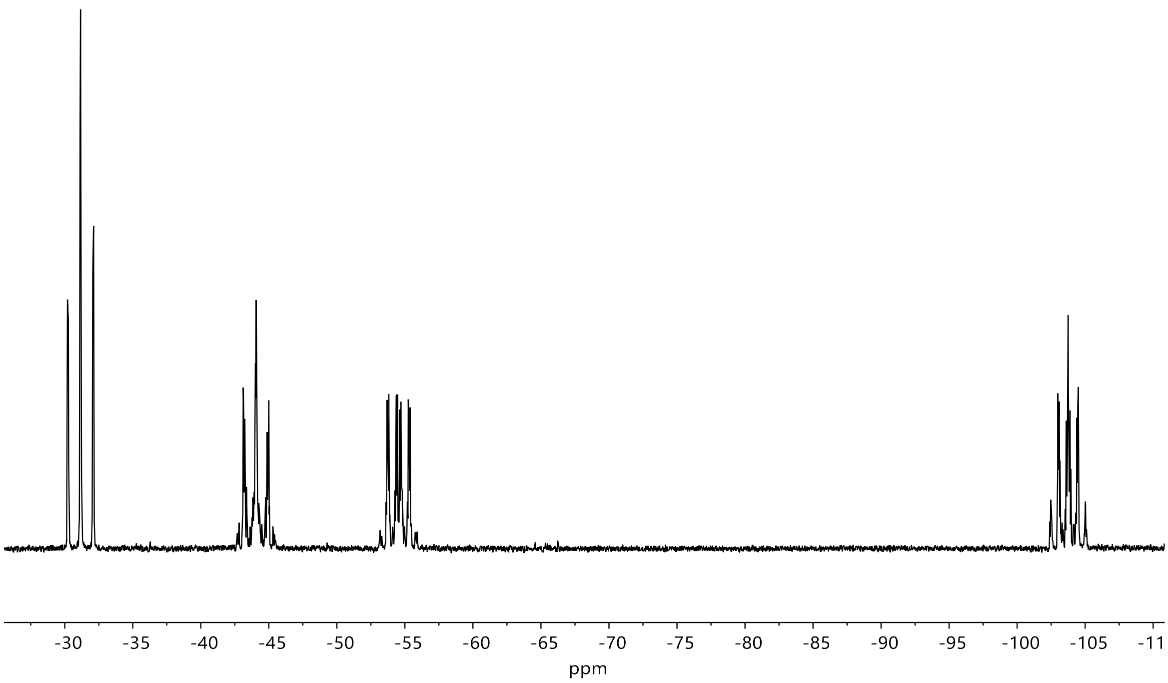

Fig. S35 $^{31}P\{^1H\}$ NMR spectrum of **8** at 162 MHz (ns = 11021).

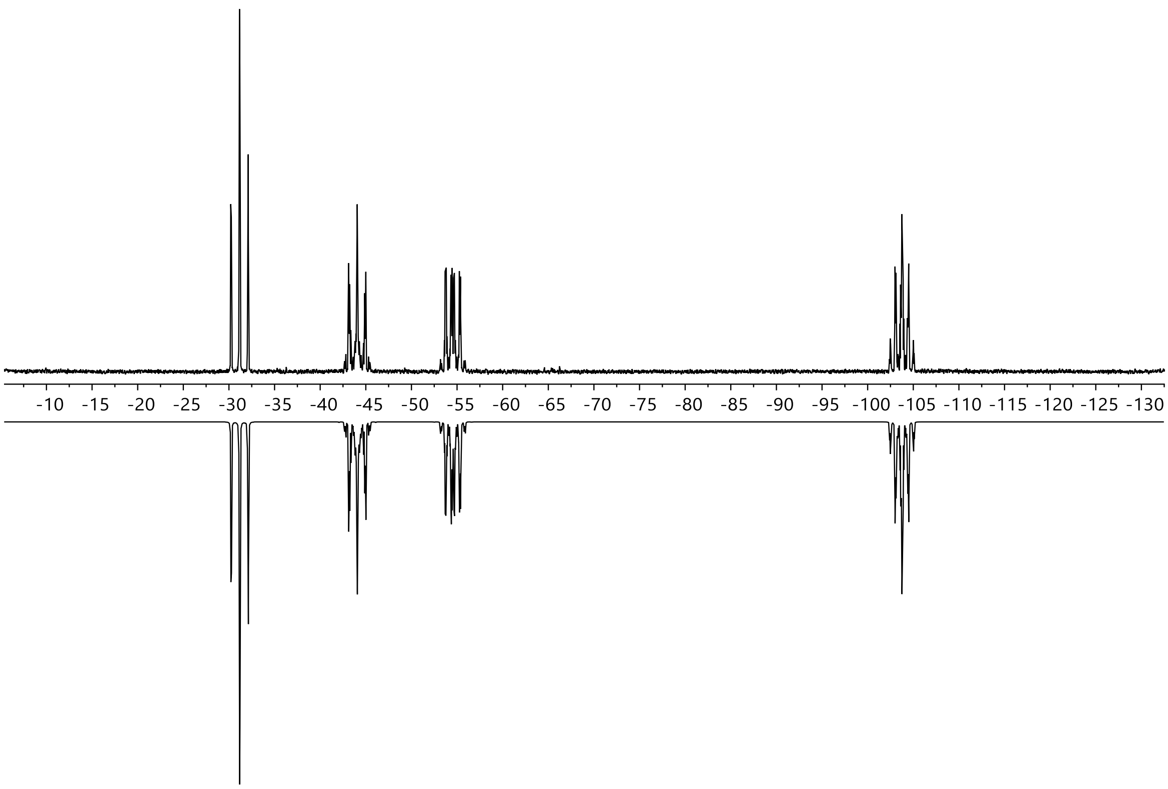

Fig. S36 Experimental (top) and simulated (bottom) $^{31}P\{^1H\}$ NMR spectrum of **8** at 162 MHz.

3.9. *cyclo*-{$P_4{}^tBu_3(SiMe_3)$}

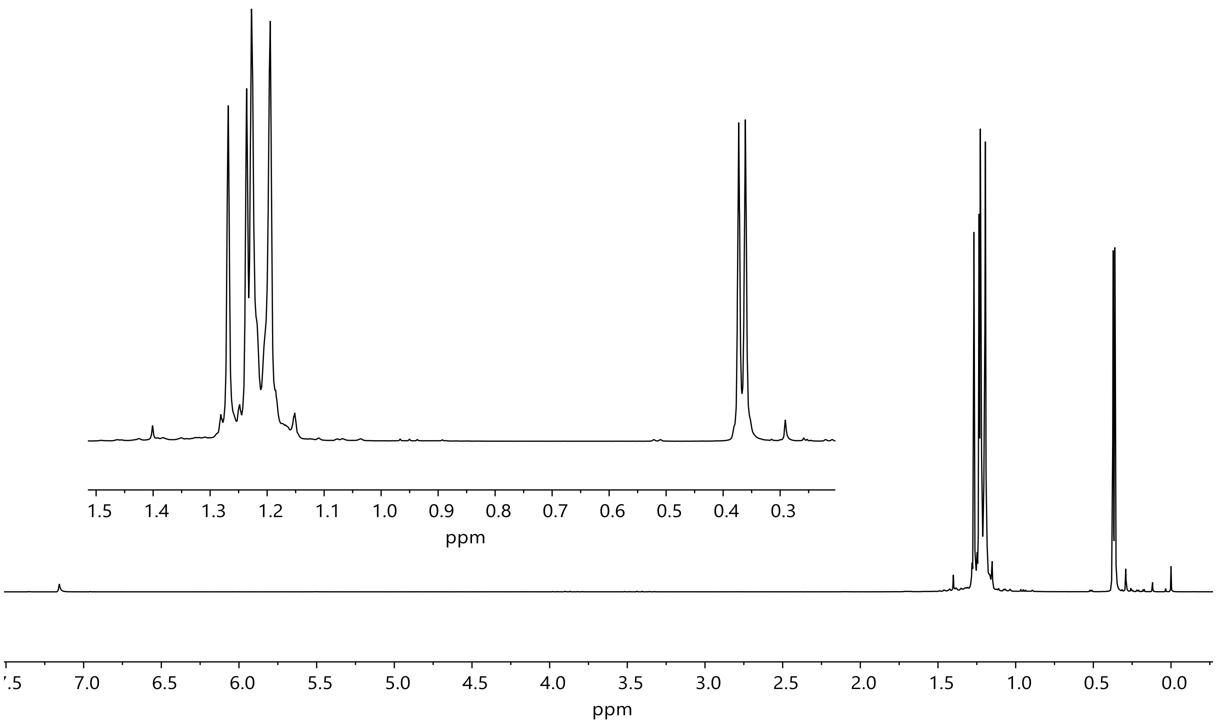

Fig. S37 ^{1}H NMR spectrum of *cyclo*-{$P_4{}^tBu_3(SiMe_3)$} at 400 MHz.

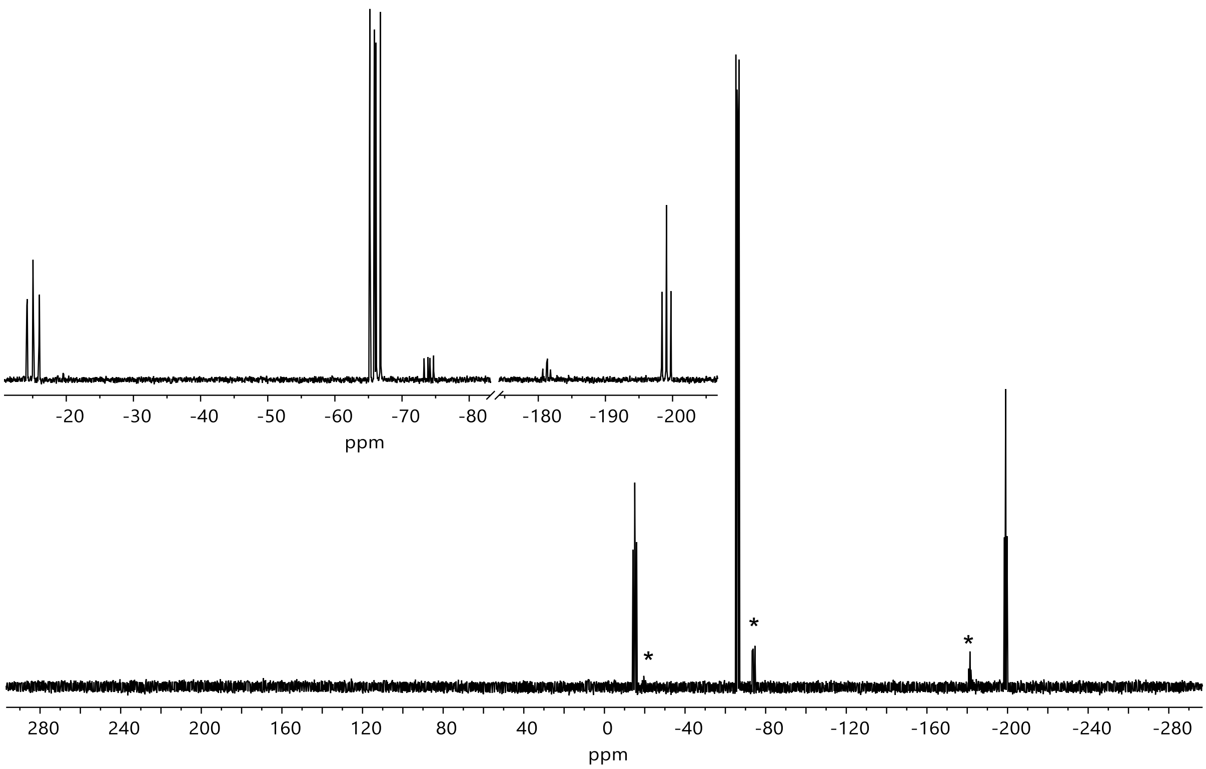

Fig. S38 ^{31}P{^{1}H} NMR spectrum of *cyclo*-{$P_4{}^tBu_3(SiMe_3)$} at 162 MHz. * = *cyclo*-{$P_4{}^tBu_3H$}.

4. References

1 G. Fritz, J. Härer and K. Stoll, Untersuchungen zur Metallierung der Cyclophosphane $P_4(Cme_3)_3(Sime_3)$, $P_4(Cme_3)_2(Sime_3)_2$, $P_4(Sime_3)_4$, *Z. Anorg. Allg. Chem.*, 1983, **504**, 47.

2 M. Baudler, J. Hellmann, P. Bachmann, K.-F. Tebbe, R. Fröhlich and M. Fehér, tBu$_6$P$_8$ and tBu$_6$As$_8$ — Two New Element-Homologous Bicyclic Compounds of Different Structure, *Angew. Chem., Int. Ed. Engl.*, 1981, **20**, 406.

3 M. Baudler, M. Schnalke and C. Wiaterek, Beiträge zur Chemie des Phosphors. 202. Hepta-*tert*-butyl-nonaphosphan(7), $P_9(t\text{-Bu})_7$, und Octa-*tert*-butyl-decaphosphan(8), $P_{10}(t\text{-Bu})_8$ Darstellung und ^{31}P-NMR-spektroskopische Strukturbestimmung, *Z. Anorg. Allg. Chem.*, 1990, **585**, 7.

4 M. Baudler, J. Hahn, H. Dietsch and G. Fürstenberg, Beiträge zur Chemie des Phosphors. 68. Tri-*t*-butyl-cyclotriphosphan, *Z. Naturforsch., B: Anorg. Chem., Org. Chem.*, 1976, **31b**, 1305.

5 K. Issleib and M. Hoffmann, Alkali-Phosphorverbindungen und ihr reaktives Verhalten. XLI. Tetra-tert.-butyl-biphosphin und Tetra-tert.-butyl-cyclotetraphosphin, *Chem. Ber.*, 1966, **99**, 1320.

6 M. Baudler, Y. Aktalay, K.-F. Tebbe and T. Heinlein, tBu$_4$P$_6$, a Novel Bicyclic Organophosphane, *Angew. Chem., Int. Ed. Engl.*, 1981, **20**, 967.

7 M. Baudler, M. Michels, J. Hahn and M. Pieroth, P$_7$$tBu_5$ – The First Bicyclo[3.2.0]heptaphosphane, *Angew. Chem., Int. Ed. Engl.*, 1985, **24**, 504.

8 T. Grell and E. Hey-Hawkins, Unexpected Isomerization of Hexa-*tert*-butyl-octaphosphane, *Chem. – Eur. J.*, 2020, **26**, 1008.